Abstract

The aim of anti-windup compensation is to modify the dynamics of a control loop when control signals saturates, so that a good transient behaviour is attained after desaturation.

Model-based anti-windup compensation is here considered for both single-input single-output(SISO) and multiple-input multiple-output(MIMO) systems. Open-loop systems are, in this report, assumed to be stable or marginally stable while nominal feedback controllers may be unstable. Systems and nominal feedback controllers are assumed to be descibed by models given in input-output form, with transfer function matrices parameterized by rational fractions. A modified controller structure is proposed, which leaves the nominal closed-loop dynamics unchanged as long as none of the control signals saturate. The loop gain around the saturation can be adjusted by designing a special anti-windup compensation transfer-function matrix. Two approaches for the design of MIMO anti-windup compensation are developed.

One is based on a fully crosscoupled MIMO system, whereas the other approach is applicable for control systems which utilize decoupling. Both approaches are generalizations of the systematic anti-windup design procedure developed by Sternad and Rönnbäck for scalar systems. The proposed design methodology strives to attain two partly contradictory goals. First, the transient effect after control signal desaturation should be small, as measured by the H_2 norm of a linear transfer function. Second, the risk of repeated re-saturation and nonlinear oscillations should be eliminated.

The main idea behind the MIMO approaches in the present report, is to reduce MIMO design to a set of scalar designs, by diagonalizing the loop gain around the control signal saturation elements. As in the scalar case, the design equations will then consist of scalar spectral factorizations. The multivariable approach is completely general and since it is based on rational fractions, it will be applicable to continuous-time systems as well as discrete-time systems. A number of examples are investigated for the decoupling approach and in this framework different design choices are evaluated.

Contents

Chapter 1

Introduction

Many of the frequently used feedback design techniques are based on linear process models. Real processes are however nonlinear in general. The nonlinearities can be either dynamic or static. One of the most frequently encountered static nonlinearities is caused by actuator saturation. In this thesis, we shall restrict the attention to static nonlinearities caused by actuator saturation.

Let us assume that a linear, nominal, feedback controller has been adjusted to control the linear dynamics of a single-input plant. Figure 1.1 depicts nominal control of a plant with a saturating actuator. Here v is the actual input to the plant which may vary between v_{max} and v_{min}.

As an example consider a valve which controls the flow of a liquid in a pipe. To keep the flow at a desired value it may happen that the regulator commands the valve to open up more than is physically possible due to its construction. A nominal linear controller will not be able to detect that the control signal saturates and it may continue to command the valve to open up even more. Since the control commands will not effect the real process when the valve saturates, the controller states will deviate from their appropriate values; they are said to "windup". When the control error finally becomes zero, the wound up controller states might cause a saturation of the control signal in the opposite direction. The valve will then close and the nominal controller will, of course, not detect this saturation either. In a worst case senario, the system could be trapped in a vicious circle, with repeated control signal saturations.

Provided that v_{min} and v_{max} are known, these saturation effects could be reduced by the use of a controller, which calculates and updates its states by using the true control signal $v \ \epsilon \ [v_{min}, v_{max}]$ instead of the assumed control output u. Such a controller will receive information of a saturation event as soon as it occurs. The controller can then be designed to react in an appropriate way when the

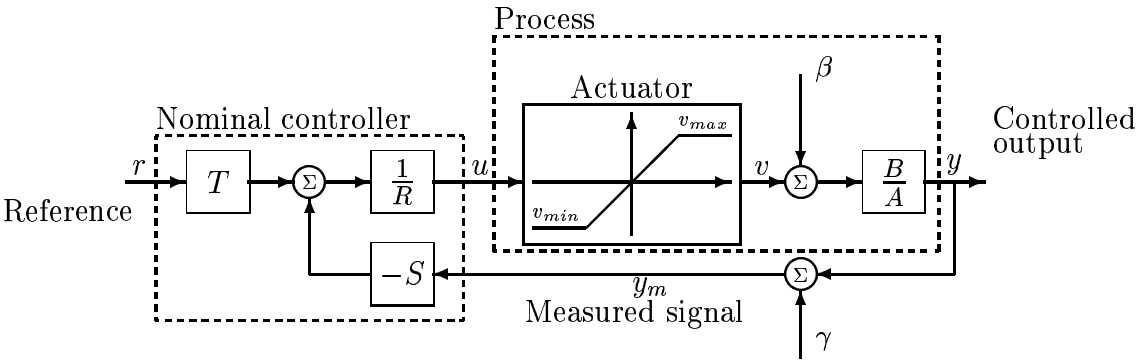

Figure 1.1: A nominal linear controller connected to a linear SISO process with actuator constraints. The signal β is a process disturbance and γ is measurement noise. The dynamics of the controller and of the process is here represented by the polynomials R, S, T, A and B, as described, for example, in [1].

control signal goes into saturation.[1]

In the example of the valve, this means that, if the valve is wide open, the modified controller will not try as hard as a nominal controller to open it any futher. When the control error indicates that the flow should be decreased, the modified controller will start to choke the valve earlier than a "nominal" controller would have done.

But, is "earlier" sufficently early? How fast will the effect of the saturation decay? Even though the saturated control signal is fed back to the controller, it will not be possible to exclusively control and modify the controller states, when the control signal saturates, without also effecting the control signal after the saturation event.

The problem of finding controllers which have desired properties during or after saturation events, has over the years resulted in a number of different anti-windup strategies. See for instance the observer-based design proposed by Åström and Wittenmark in [1], and the conditioning technique developed by Hanus and co-workers in [2]. A common property of the strategies suggested in [1][2] is that a separate anti-windup compensator is designed. This compensator is disconnected form the system as long as the actuator does not saturate. A nominal regulator can then be designed as usual, i.e. under the assumption that the system is linear, in order to give the system desired dynamic properties, as long as the control signal amplitude remains in the linear range. More information about references to this subject is to be found in the PhD thesis [3] by Rönnbäck.

For reasons explained in [4], and afterwards also investigated and decribed in [5][3], there is, however, no guarantee that the whole system behaves acceptably,

[1]Systematic anti-windup compensation schemes for systems with both actuator magnitude constraints and actuator rate constraints would be of value in several practical applications. We will, however, not consider such situations in this thesis.

during or after a saturation event, even though we have prevented *controller*-state windup. Nonlinear oscillations and even limit cycles might occur. To avoid such effects, the whole linear dynamics around the saturating element, consisting of nominal controller elements, anti-windup filters and the open-loop plant, have to be taking into account. This can be done by the use of a Nyquist-like design method suggested by Wurmthaler and Hippe in [4].

One drawback of this method is that it is based on a re-design of the nominal linear controller. The anti-windup modification proposed in [4] influence the dynamic properties of the system even when the actuator does not saturate.

An anti-windup compensator structure which adds sufficient degees of freedom to the system in order to use ideas similar to those suggested in [4] without having to modify the nominal design, is suggested in [5]([3](Part II)). Futhermore, this proposed compensator will only modifiy the dynamics of the closed loop when the actuator (control signal) saturates. With this modified controller, it becomes possible to exclusively control the dynamics of desaturation transients. A Nyquist-like method based on H_2-optimization for the design of this compensator is suggested in [6]([3] Part VII).

The structural modification of controllers for Single Input-Single Output(SISO) systems, operating under actuator constraints, is briefly described in Chapter 2. The modification of the controller is based on the work by Rönnbäck [3] and Rönnbäck, Walgama and Sternby [5]. The design of the anti-windup compensator is based on the work by Rönnbäck and Sternad [6]. In the subsequent chapters, these ideas are generalized for use in Multiple-Input Multiple-Output(MIMO) systems with actuator constraints. The anti-windup compensated controller discussed in Chapter 2, and the systematic anti-windup design procedure associated with such a controller, are generalized in Chapter 3, to MIMO systems.

The open-loop systems are here assumed stable or marginally stable, while nominal feedback controllers may be unstable. Systems and nominal controllers are assumed to be descibed by models given in input-output form, with transfer function matrices parameterized by rational fractions. The main idea behind the MIMO approaches in the present report, is to reduce MIMO design to a set of scalar designs, by diagonalizing the loop gain around the control signal saturation elements. A very simple and direct variant of the method, which is based on the use of feedforward decoupling in the nominal controller design, is presented in Chapter 4. At the end of this report, a number of designs are tested on a model of a Heavy Oil Fractionator process. The feedforward decoupling regulator is used in all these examples, with or without anti-windup compensation.

1.1 Remarks on the notation

Throughout this report, only discrete time systems, with normalized sampling time, are considered. Nevertheless, theories and derivations are directly applicable to continuous-time systems. The time index is denoted k. Constant matrices are denoted by boldface roman letters, such as $\mathbf{F}$.

Polynomials in the forward shift operator q, $(qy(k) = y(k+1))$ are denoted by italic letters, such as $A(q)$ or A, with degree na.

The polynomial A^* denotes the conjugate polynomial to A, in which the forward-shift operator q is substituted by the backward operator q^{-1}.

Scalar and time-invariant discrete-time dynamic systems, described by linear difference equations

$$A(q)y(k) = B(q)u(k) \tag{1.1}$$

are represented by rational transfer operators, or transfer functions, indicated by calligraphic letters,

$$y(k) = \mathcal{H}(q)u(k) = \frac{B(q)}{A(q)}u(k) \quad . \tag{1.2}$$

The complex variable z is substituted for q whenever poles and zeros of rational transfer functions are discussed.The systems are asymptotically stable whenever $\mathcal{H}(z)$ has all its poles in $|z| < 1$. The polynomial $A(q)$ is said to be "stable", or strictly Schur, when all zeros of $A(z)$ are located within the unit circle $|z| = 1$. The polynomial $A(q)$ is said to be "marginally stable", when there are zeros of $A(z)$ located on the unit circle $|z| = 1$.

Polynomial *matrices* will be denoted as

$$\boldsymbol{A}(q) = \mathbf{A}_0 q^{na} + \mathbf{A}_1 q^{na-1} + \ldots + \mathbf{A}_{na} \tag{1.3}$$

with $\boldsymbol{A}_i$ representing the coefficient matrices.

The notation $\boldsymbol{A}^*$ denotes the conjugate-transpose of the polynomial matrix $\boldsymbol{A}$, where the backward-shift operator q^{-1} is substituted for q i.e.

$$\boldsymbol{A} = (a_{ij}(q)) : \boldsymbol{A}^* = (a_{ji}(q^{-1})) \quad , \tag{1.4}$$

or

$$\boldsymbol{A}^*(q) = \mathbf{A}_0^T q^{-na} + \mathbf{A}_1^T q^{-(na-1)} + \ldots + \mathbf{A}_{na}^T \quad . \tag{1.5}$$

The degree of a polynomial matrix $\boldsymbol{A}$, denoted by na, is defined as the highest degree of any of its polynomial elements. Futhermore, $\boldsymbol{A}(q)$ is said to be *monic* if the leading coefficient matrix $\mathbf{A}_0$ above equals the identity matrix.

Matrix transfer operators, or *rational matrices*, have transfer operators as elements. They will be denoted by boldface calligraphic letters, like $\boldsymbol{\mathcal{A}}(q)$. Rational matrices are said to be *proper* if all of their elements have numerator degrees not higher than the denominator degrees. They then represent causal difference equations. Arguments of polynomials and polynomial and rational matrices will be omitted when there is no risk of misunderstanding.

Multivariable discrete-time systems, described by matrix transfer functions, are asymptotically *stable* if and only if all of their transfer function elements have poles only within the unit circle $|z| = 1$. Square polynomial matrices $\boldsymbol{A}(q)$ will be said to be stable if all zeros of the determinant polynomial $\det(\boldsymbol{A}(z))$ are located within the unit circle $|z| = 1$.

Let $Y(C)$ denote the *describing function*, cf. [7][8], of a saturation nonlinearity. The argument C is an amplitude of an sinusoid which, if it is precent, may exite nonlinear dynamics in the closed loop. We shall call the function

$$\frac{-1}{Y(C)} \tag{1.6}$$

the *NonLinearity Characteristic Function (NLCF).* The loop gain around the nonlinearity, denoted by $\mathcal{L}_v(\omega)$, and the corresponding $NLCF$, is depicted in a Nyquist diagram below.

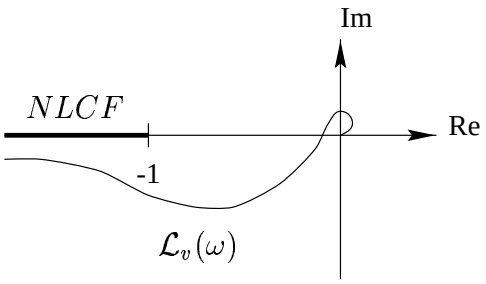

Chapter 2

Anti-Windup Compensators for Scalar Control Systems

As a prerequisite for the design of MIMO anti-windup compensators we shall in this chapter review the anti-windup compensator design technique developed in [5][3][6] for scalar systems.

2.1 Scalar anti-windup controller design

Let the process to be controlled be described by a linear input-output model expressed in polynomial form

$$y(k) = \frac{B(q)}{A(q)} v(k) + \beta(k) \;\; ; \;\; v(k) = \text{sat}[u(k)]_{v_{min}}^{v_{max}} \;, \tag{2.1}$$

where $\beta(k)$ is an input disturbance. If the system is open-loop unstable, it will not be possible, for all initial conditions, to prevent the output signal from growing towards infinity whenever the control signal is saturated. Marginally stable systems can be stabilized by saturating control elements, see [8]. Let us therefore in the following assume the open-loop system to be stable or marginally stable. In other words, the denominator polynomial $A(z)$ has zeros within, or on, the unit circle $|z| = 1$.

The nominal controller is given by the linear difference equation

$$R(q)u(k) = -S(q)y_m(k) + T(q)r(k) \;; \;\; y_m(k) = y(k) + \gamma(k) \tag{2.2}$$

where $r(k)$ is the reference signal, $y(k)$ is the measured output signal from the plant, and $u(k)$ is the unsaturated control signal. The polynomials $R(q)$ and $A(q)$ are assumed monic. The nominal control structure is depicted in Figure 1.1. For

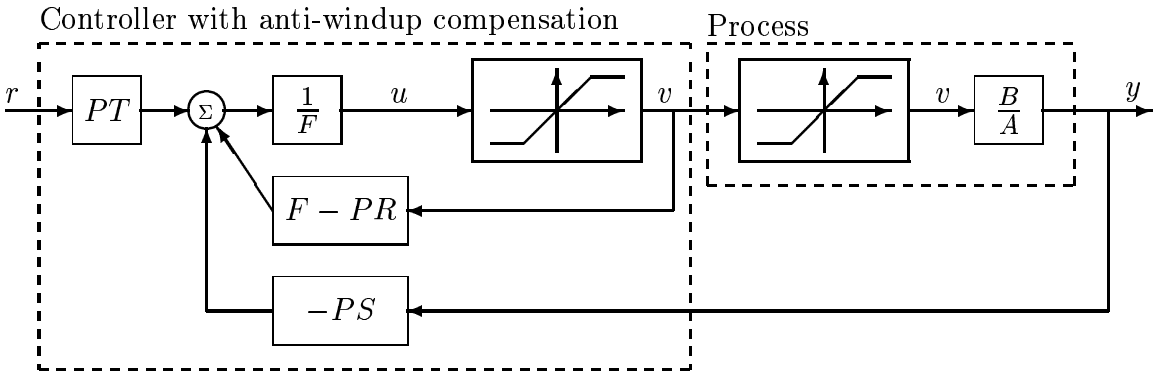

Figure 2.1: Anti-windup compensation of the nominal controller in Figure 1.1. A model of the saturation is used to feed the saturated control signal back to the controller. This modified controller structure has been suggested by Rönnbäck *et.al.* in [5].

simplicity we shall in the sequel neglect the influence of the disturbance β, and of the measurement noise γ. Thus,

$$y_m(k) = y(k) = \frac{B}{A}v(k) \quad . \tag{2.3}$$

We shall also assume that the saturated control signal $v(k)$ is known, either from measurements, or from a model of the saturation. The saturation limits v_{min} and v_{max} may be time dependent.

A modification of the nominal controller structure (2.2), which was suggested in [5] and [6], for controlling saturation events, will now be presented. To prevent undesired effects caused by control signal saturation, it is crucial that the saturated control signal $v(k)$ is fed back to the controller. One simple way to take the true control signal $v(k)$ into account is to let delayed values of the saturated control signal $v(k)$ be utilized instead of delayed values of $u(k)$ in the controller recursion (2.2). We would then obtain the modified controller

$$q^{nr}u(k) = (q^{nr} - R)v(k) - Sy(k) + Tr(k) \quad . \tag{2.4}$$

Notice that (2.4) is identical to (2.2) whenever $v(k-i) = u(k-i)$ for $i = 1, \ldots nr$.

By appending two additional stable and monic polynomials $F(q)$ and $P(q)$ to (2.4), a more general controller structure can be introduced as

$$\begin{aligned} Fu(k) &= (F - PR)v(k) - PSy(k) + PTr(k) \\ v(k) &= \text{sat}[u(k)]_{v_{min}}^{v_{max}} \quad . \end{aligned} \tag{2.5}$$

A block diagram of the resulting controller structure is shown in Figure 2.1. Observe that when $F(q) = q^{nr}, P(q) = 1$, the difference equation (2.5) is identical to (2.4). To avoid algebraic loops around the saturation, it must be assumed that

$$nf = np + nr \quad . \tag{2.6}$$

The difference equation and the saturation model (2.5) together, represent a variable-structure controller. By appropriate choices of the polynomials $F(q)$ and $P(q)$, it becomes possible to influence the controller behavior during and after saturation events. The closed-loop dynamics for non-saturating control signals will remain unchanged, and will be determined by R, S, A and B. Notice that the input-output properties of (2.5) are identical to those of (2.2) whenever $v(i) = u(i)$, for $i = 0, 1...nr$. When $v(k) \neq u(k)$, the control system will react on the difference between the unsaturated control signal u and the saturated control signal v, in a way determined by the "anti-windup polynomials" P and F. In [1], one method of anti-windup compensation, called *The observer-based method*, is suggested and outlined. This method corresponds to the choice $P = 1$ in 2.5, and a choice of $F(q)$, of degree nr, as a stable "windup observer" polynomial. The anti-windup compensated controller, structure 2.4 obtained from the choice $F(q) = q^{nr}, P(q) = 1$ in (2.5) can be obtained as a special case of the observer-based method. Such an observer is called a *deadbeat observer*, and the compensator is denoted a *deadbeat anti-windup compensator*.

Some insight into the consequences of different choices of $F(q)$ and $P(q)$ in (2.5) can be obtained by an approximate linear analysis. Let $\delta(k)$ denote the difference between $v(k)$ and $u(k)$, that is

$$\delta(k) \;=\; v(k) - u(k) \;=\; \mathrm{sat}[u(k)]_{v_{min}}^{v_{max}} - u(k) \quad . \tag{2.7}$$

Now, $\delta(k)$ can be interpreted as a disturbance acting on the system, cf. Figure 2.2. A simplified description of the effect of the nonlinearity can be obtained by neglecting the nonlinear dependence of $\delta(k)$ on $u(k)$, i.e. by regarding $\delta(k)$ as an exogenous disturbance. For more details on the use and the limitations of such an intepretation, see [6]. We may use $\delta(k)$ to describe the transient response of the system when the control signal exits saturation. The effect of $\delta(k)$ on the system will then correspond to an initial value decay, influenced by the additional polynomials P and F. As long as the control signal does not resaturate, the whole closed-loop system will remain linear. If the effect of the nonlinearity is represented by an equivalent disturbance acting on the input to the plant, that is, by

$$v(k) = u(k) + \delta(k) \tag{2.8}$$

then the output signal $y(k)$ of Figure 2.1 can be described as being determined by two transfer functions, one from the reference signal $r(k)$ and the other one

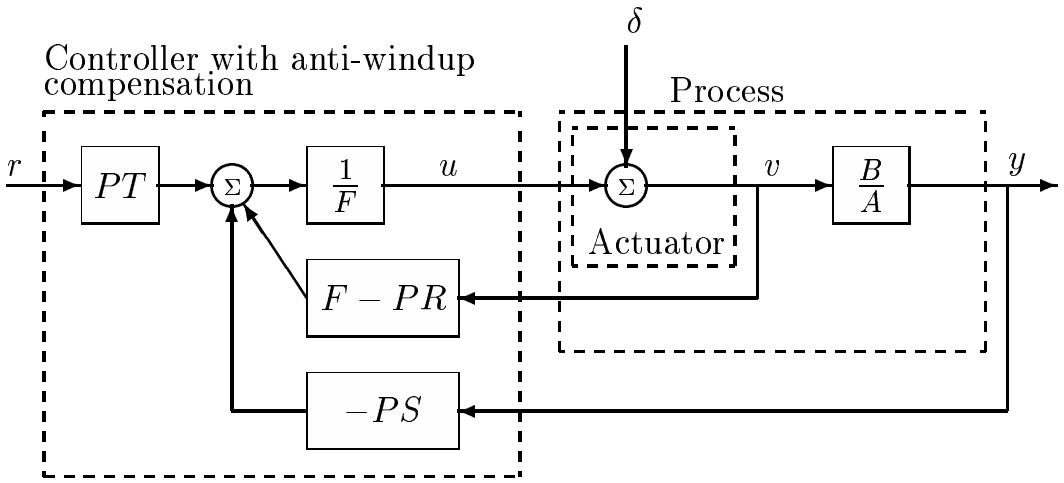

Figure 2.2: System with anti-windup compensated controller. The difference between the saturated control signal $v(k)$ and the unsaturated control signal $u(k)$ is modeled as a disturbance $\delta(k)$.

from $\delta(k)$. The output signal $y(k)$ is then obtained as

$$y(k) \;=\; y_{nom}(k) + y_\delta(k) \tag{2.9}$$

where

$$y_{nom}(k) \;=\; \mathcal{H}_{nom} r(k) \;=\; \frac{BT}{\alpha} r(k) \tag{2.10}$$

$$y_\delta(k) \;=\; \mathcal{H}_\delta \delta(k) \;=\; \frac{BF}{P\alpha} \delta(k) \tag{2.11}$$

and where

$$\alpha(q) \;=\; R(q)A(q) + S(q)B(q) \tag{2.12}$$

represents the characteristic polynomial of the nominal closed loop system.

The dynamics controllable from $r(k)$ is represented by $\mathcal{H}_{nom}(q)$ which is unaffected by $F(q)$ and $P(q)$. The modes excited by $\delta(k)$ have dynamic properties corresponding to $\mathcal{H}_\delta(q)$. In order to alleviate the effect of saturation, the polynomials $P(q)$ and $F(q)$ of $\mathcal{H}_\delta(q)$ have to be selected carefully. It might be tempting to select $F(q)$ and $P(q)$ so that the dynamics of $\mathcal{H}_\delta(q)$ becomes "fast". However, due to the inherently nonlinear feedback, which is not apparent by regarding $\delta(k)$ as an exogenous disturbance, such a choice may cause stable-cycle oscillations and repeated re-saturations when the control signal saturates. These effects can be explained by investigating the relative locations of the *NonLinearity Characteristic Function (NLCF)* (1.6), and the loop gain around the nonlinearity. See [4][6].

If this loop gain is located too close to the NLCF, then repeated re-saturations and oscillating transients may be present. If the loop gain intersects with the NLCF, stable cycle oscillations may occur. The loop gain around the saturation of the system depicted in Figure 2.1 is

$$\mathcal{L}_v = \frac{P\alpha}{FA} - 1 \quad . \tag{2.13}$$

Considering (2.11) and (2.13), a qualitative conclusion can be drawn: Because $\mathcal{H}_\delta$ is proportional to F/P while the first term of $\mathcal{L}_v$ is proportional to P/F, the use of P and F to reduce the gain of $\mathcal{H}_\delta$, will increase the loop gain $\mathcal{L}_v$. This may force this function to approach and to cross the NLCF, with repeated resaturations or limit cycle oscillations as a result. Consequently, there is a trade-off between minimizing $\mathcal{H}_\delta$ and keeping the loop gain away from the NLCF.

2.2 Systematic anti-windup design

Different ways to describe the saturation and the different approaches to compensate for it, have over the years resulted in suggestions for a number of anti-windup design methods. See [1],[2],[5],[3][6][4]. It is possible to interprete these and other methods in terms of special choices of the polynomials F and P [5][6]. Examples include the *Conditioning technique* by Hanus [2], and *The observer based approach* by Åström and Wittenmark [1].

Throughout this report we shall use a method which will be called *Systematic anti-windup design*. It was developed in [6], and has been motivated by the trade-off between minimizing $\mathcal{H}_\delta$ and forcing the loop gain $\mathcal{L}_v$, introduced in (2.13), away from the NLCF. The systematic anti-windup design method is formulated as an optimization problem.

The idea is to determine $P(q)$ and $F(q)$, which are factors of both $\mathcal{H}_\delta$ and $\mathcal{L}_v$, by minimizing the criterion function

$$\begin{aligned} J &= \| \mathcal{H}_\delta \|_2^2 + \rho \| \left(\mathcal{L}_v + 1\right)^{-1} - 1 \|_2^2 \\ &= \left\| \frac{BF}{P\alpha} \right\|_2^2 + \rho \left\| \frac{AF}{P\alpha} - 1 \right\|_2^2 \end{aligned} \tag{2.14}$$

where the scalar ρ plays the role of a trade-off parameter. If ρ is selected as a small number, then the result will tend to minimize the H_2-norm of the desaturation dynamics $\mathcal{H}_\delta$, whereas a large value of ρ ensures that the loop gain stays well away from the NLCF. As a matter of fact, the loop gain $\mathcal{L}_v$ collapses towards a point at the origin if ρ is increased.

The solution to the minimization of the criterion (2.14) is obtained by solving a linear polynomial equation and a spectral factorization equation [6]. The linear polynomial equation is solved by the choice $F(q) = \alpha(q)$ and since $\alpha(q)$ is monic and stable, such an assignment is always admissible.

$$\boxed{F = \alpha = RA + SB} \tag{2.15}$$

The optimal choice of the stable and monic polynomial $P(q)$ is then obtained from the polynomial spectral factorization equation

$$\boxed{rPP^* = BB^* + \rho AA^*} \quad . \tag{2.16}$$

Here, r is a scale factor and A^* denotes the conjugate polynomial

$$A^*(q^{-1}) = q^{-na} + a_1 q^{-na+1} + \ldots + a_{na} \quad . \tag{2.17}$$

2.3 The systematic anti-windup design procedure for scalar systems

Assume that the plant is given by (2.1) and the controller by (2.5). Then the criterion (2.14), and the design equation (2.16), can be used to adjust the windup properties of the resulting closed-loop system.

A convenient way to do this is to use a multi-step procedure, see [6] for details, which presupposes the following requirements.

1. The plant must be open-loop stable or marginally stable, and a transfer function model 2.1 of the plant is assumed known.

2. The saturated control signal $v(k)$ must be known at all times k, either from measurements, or from a model of the saturation.

3. A pre-existing nominal controller is assumed to be given in input-output form 2.2. The nominal closed-loop behaviour (without saturation) is to remain unchanged.

Step one

Append the anti-windup design polynomials F and P to the nominal controller (2.2) and use the saturated control signal $v(k)$ to create a control law equal to (2.5). Figure 2.1 illustrates the structure of the modified controller.

Step two

Set F equal to $\alpha = AR + SB$ as in (2.15). Select a penalty ρ, and solve the spectral factorization (2.16) for P. Plot the loop gain $\mathcal{L}_v(\omega)$ defined by (2.13) and $-1/Y(C)$ (where $Y(C)$ is the describing function of the saturation nonlinearity), in a Nyquist diagram.

Step three

If required, adjust the parameter ρ to obtain a more suitable loop gain, $\mathcal{L}_v(\omega)$ and repeat step 2.

Step four

Simulate the system with saturating control signals and different types of disturbances. If the result is not satisfying, go through steps two and three again.

For system and controller combinations with stable loop gains, the parameter ρ is increased in step 2 and 3, from an initial small value, until the loop-gain locus $\mathcal{L}_v(\omega)$ is close, but not too close, to the line $-1/Y(C)$ which starts at -1 and goes towards infinity along the negative real axis of the complex plane. Criteria for suitable closeness between these two curves are discussed in [4] and in [6]. A simple cone around $-1/Y(C)$, with opening to the left and an opening angle of 80^o is suggested in [4]. The use of a more elaborate signal-dependent safety margin around the loop gain $\mathcal{L}(\omega)$ is suggested in [6].

For loop gains $\mathcal{L}_v$ containing multiple integrators, it will be impossible to avoid one or several crossings between $\mathcal{L}_v(\omega)$ and $-1/Y(C)$. Some of these intersections indicate that stable limit cycle oscillations will occur, if an excitation of sufficiently large amplitude is introduced. The frequency ω of $\mathcal{L}_v(\omega)$ and the amplitude C of $-1/Y(C)$, corresponding to the intersection point, indicate the properties of the resulting stable oscillations. The design strategy will in such a case be focused on shifting the unavoidable intersection points to regions along the NLCF, where the corresponding amplitude is so high, so that no realistic disturbance in the system could cause oscillations.

Chapter 3

Anti-Windup Compensators for Multivariable Control Systems

The main purpose of this thesis is to find a way to introduce Anti-Windup Compensators into multivariable systems, and to use the method of *Systematic Anti-Windup design* to form this AWC filter. In this chapter, we will suggest a solution to this problem.

The method of Systematic Anti-Windup design for SISO systems is based on a Nyquist-like design procedure, where the loop gain is adjusted in relation to the NLCF (1.6). This approach can be used also for MIMO systems if the loop gain around the saturations is made diagonal. Such a restriction allows us to independently analyze and adjust the loop gains around each individual saturating actuator. The design of a multivariable anti-windup compensator can then be reduced to a set of scalar designs.

3.1 MIMO representation of the process model and of the nominal controller

The dynamic properties of a multivariable system

$$y(k) = \boldsymbol{\mathcal{H}}(q)v(k) \tag{3.1}$$

are given by the proper elements of the transfer-operator matrix $\boldsymbol{\mathcal{H}}(q)$. In analogy to the scalar case, $\boldsymbol{\mathcal{H}}(q)$ can be parameterized by a *matrix* fraction, as

$$\boldsymbol{\mathcal{H}}(q) = \boldsymbol{B}(q)\boldsymbol{A}^{-1}(q) \tag{3.2}$$

where $\boldsymbol{B}(q)\boldsymbol{A}^{-1}(q)$ is a right matrix-fraction form of $\boldsymbol{\mathcal{H}}(q)$. Left fractions are defined analogously. If $\boldsymbol{B}(q)$ and $\boldsymbol{A}(q)$ both are polynomial matrices then $\boldsymbol{B}(q)\boldsymbol{A}^{-1}(q)$ is called a right *Matrix Fraction Description*(MFD) of $\boldsymbol{\mathcal{H}}(q)$ [9][10].

If $\boldsymbol{\mathcal{H}}(q)$ is parameterized as

$$\boldsymbol{\mathcal{H}}(q) = \boldsymbol{\mathcal{B}}(q)\boldsymbol{\mathcal{A}}^{-1}(q) \tag{3.3}$$

where $\boldsymbol{\mathcal{B}}(q)$ and $\boldsymbol{\mathcal{A}}(q)$ both are stable and proper transfer-operator matrices, then $\boldsymbol{\mathcal{B}}(q)\boldsymbol{\mathcal{A}}^{-1}(q)$ is called a right *rational fractional representation* of $\boldsymbol{\mathcal{H}}(q)$ [9][10].

Rational fractional representations will be utilized to represent systems and regulators in this chapter, mainly for three reasons.

1. In the same way as with the use of polynomial fractions in q^{-1}, the use of proper rational fractions in q will guarantee the causality of systems interacting in open and closed loop. Proper rational fractions in q do, in fact, include polynomial fractions (MFDś) in q^{-1} as a special case,

   $$\boldsymbol{\mathcal{H}}(q) \;=\; \boldsymbol{\mathcal{B}}(q)\boldsymbol{\mathcal{A}}^{-1}(q) \;=\; \boldsymbol{B}(q^{-1})\boldsymbol{A}^{-1}(q^{-1}) \quad ,$$

   if the denominators of the rational elements are selected as q^n, with n selected appropriately. For example,

   $$\frac{q-2}{q^2-0.8q+0.4} = \frac{\dfrac{q-2}{q^2}}{\dfrac{q^2-0.8q+0.4}{q^2}} = \frac{q^{-1}-2q^{-2}}{1-0.8q^{-1}+0.4q^{-2}} \quad .$$

2. While developed in discrete time, the use of proper and stable rational fractions allows the AWC-design theory to be applied directly also in continuous time[1]

3. Rational representation of regulators (see (3.7) below) will facilitate the inclusion of a large class of pre-existing MIMO controller structures. For example, observer-based state-feedback regulators, where the stable observer dynamics will play the role of stable denominators in the rational functions.

Let a MIMO generalization of the plant (2.1) have m inputs and p outputs. We will parameterize the plant model by a right fractional representation in the sequel. In order to simplify the discussed design procedures and realizations involved in the systematic anti-windup concept, we shall use a diagonal denominator matrix $\boldsymbol{\mathcal{A}}(q)$ in the fractional representation of the plant model. The

[1] In the continuous-time case, the derivativ operator p is substituted for q, s is substituted for z and the stability area corresponds to the left-half plane. Thus, $\boldsymbol{\mathcal{B}}$ and $\boldsymbol{\mathcal{A}}$ in e.g. $\boldsymbol{\mathcal{H}}(s) = \boldsymbol{\mathcal{B}}(s)\boldsymbol{\mathcal{A}}^{-1}(s)$ must have proper elements, which poles have to be located stricly in the left half plane. In conjugate polynomials $\boldsymbol{\mathcal{A}}^*$, $-s$ is substituted for q^{-1}.

numerator matrix $\boldsymbol{\mathcal{B}}(q)$ is assumed to be a full transfer-operator matrix. We thus obtain

$$y(k) = \boldsymbol{\mathcal{B}}(q)\boldsymbol{\mathcal{A}}^{-1}(q)v(k) = \boldsymbol{\mathcal{H}}(q)v(k) \tag{3.4}$$

or

$$\begin{pmatrix} y_1(k) \\ \vdots \\ y_p(k) \end{pmatrix} = \begin{pmatrix} \mathcal{B}_{11} & \dots & \mathcal{B}_{1m} \\ \vdots & & \vdots \\ \mathcal{B}_{p1} & \dots & \mathcal{B}_{pm} \end{pmatrix} \begin{pmatrix} \mathcal{A}_1 & & \mathbf{0} \\ & \ddots & \\ \mathbf{0} & & \mathcal{A}_m \end{pmatrix}^{-1} \begin{pmatrix} v_1(k) \\ \vdots \\ v_m(k) \end{pmatrix} \tag{3.5}$$

$$, \tag{3.6}$$

where all elements of $\boldsymbol{\mathcal{B}}$ and $\boldsymbol{\mathcal{A}}$ are stable and proper. We shall, as in the previous chapter, not include disturbances ($\beta(k) = \gamma(k) = 0$ in Figure 1.1) in the discussion.

In the following, whenever a multivariable controller

$$\boldsymbol{\mathcal{R}}(q)u(k) = -\boldsymbol{\mathcal{S}}(q)y(k) + \boldsymbol{\mathcal{T}}(q)r(k) \tag{3.7}$$

is under consideration, $\boldsymbol{\mathcal{R}}(q)$, $\boldsymbol{\mathcal{S}}(q)$ and $\boldsymbol{\mathcal{T}}(q)$ are assumed to be stable and proper rational matrices of dimension $m|m$, $m|p$ and $m|p$, respectively. Assume also, as before, that the saturated control signal vector $v(k)$ is fed back into the controller. One simple way to take the true control signals $v(k)$ into account is to let delayed values of $v(k)$ be utilized instead of delayed values of $u(k)$ in the controller recursion. We would then obtain the modified controller

$$u(k) = (\mathbf{I} - \boldsymbol{\mathcal{R}})v(k) - \boldsymbol{\mathcal{S}}y(k) + \boldsymbol{\mathcal{T}}r(k) \quad . \tag{3.8}$$

It should be noted that, the expression (3.8) does *not* necessarily correspond to a MIMO dead-beat anti-windup controller, even though (2.4) does in the scalar case. This is due to the fact that $\boldsymbol{\mathcal{R}}$ is assumed to be a *rational* matrix. The denominator polynomials of the elements of $\boldsymbol{\mathcal{R}}$ will control the dynamic properties of any desaturation event and hence, this controller may already have some kind of anti-windup compensation (not necessary dead beat) contained inside its structure.

3.2 MIMO anti-windup compensation

If the equation (2.5), for the scalar controller, is divided by the stable polynomial $F(q)$, we obtain

$$u(k) = \left(1 - \frac{P}{F}R\right)v(k) - \frac{P}{F}Sy_m(k) + \frac{P}{F}Tr(k) \quad . \tag{3.9}$$

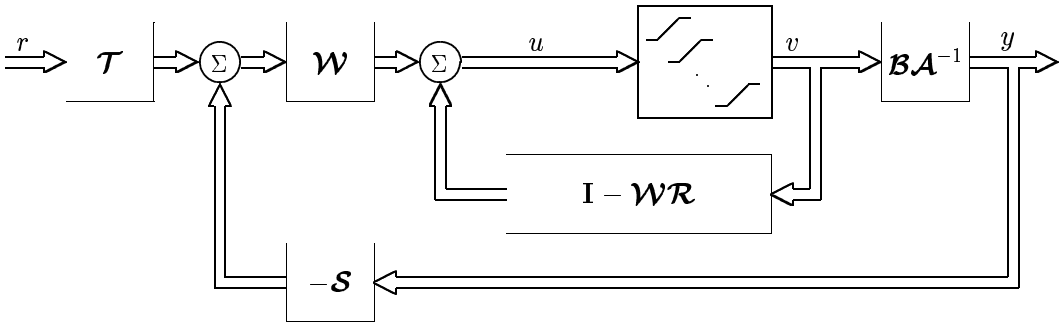

Figure 3.1: A discrete-time MIMO process $y(k) = \mathcal{B}(q)\mathcal{A}^{-1}(q)\text{sat}[u(k)]$ with a two degree of freedom controller structure $\{\mathcal{R}(q)\ \mathcal{S}(q)\ \mathcal{T}(q)\}$ appended with a stable and proper anti-windup transfer-operator matrix $\mathcal{W}(q)$. The rational matrix $\mathcal{W}(q)$ is to be designed such that the loop gain becomes diagonal and such that the desaturation transient decays as fast as possible, while avoiding repeated re-saturations.

In analogy with the above expression, the structure of a general multivariable discrete-time recursive control law, with anti-windup facilities, will be represented by

$$u(k) = (\mathbf{I} - \mathcal{WR})v(k) - \mathcal{WS}y(k) + \mathcal{WT}r(k) \quad , \tag{3.10}$$

where the stable and proper $m|m$ rational matrix $\mathcal{W}(q)$ now plays a similar role as $P(q)/F(q)$ does in (3.9). The controller (3.10), connected to a plant described by the model (3.4), is depicted in Figure 3.1.

Whenever a multivariable anti-windup compensator is under consideration, a fractional representation will be used to represent the rational anti-windup matrix $\mathcal{W}(q)$, as

$$\mathcal{W}(q) = \mathcal{P}(q)\mathcal{F}^{-1}(q) \quad . \tag{3.11}$$

For reasons described below, $\mathcal{P}(q)$ is a *diagonal* $m|m$ transfer-operator matrix, while $\mathcal{F}(q)$ is a full $m|m$ transfer-operator matrix. Futhermore, $\mathcal{P}(q)$ and $\mathcal{F}(q)$ are both assumed to be chosen stable and proper. In analogy to the scalar case we also assume $\mathcal{P}^{-1}(q)$ and $\mathcal{F}^{-1}(q)$ to be chosen stable.

Remark 3.1: Notice that $(\mathbf{I} - \mathcal{W}(q)\mathcal{R}(q))$ must be strictly proper to avoid the occurence of algebraic loops. In other words, a matrix series expansion of $\mathcal{W}(q)\mathcal{R}(q)$, with respect to q, must have a **unit** matrix as the leading term.

By making use of δ as defined in (2.7) the output $y(k)$ can, as before, be decomposed into a nominal response (caused by the reference signal) and a response which is caused by the saturation. In other words

$$y(k) = y_{nom}(k) + y_\delta(k) \tag{3.12}$$

where

$$y_{nom}(k) = \boldsymbol{\mathcal{H}}_{nom} r(k) = \boldsymbol{\mathcal{B}}\boldsymbol{\alpha}^{-1}\boldsymbol{\mathcal{T}} r(k) \tag{3.13}$$

and

$$y_\delta(k) = \boldsymbol{\mathcal{H}}_\delta \delta(k) = \boldsymbol{\mathcal{B}}\boldsymbol{\alpha}^{-1}\boldsymbol{\mathcal{W}}^{-1}\delta(k) \quad . \tag{3.14}$$

Here, $\boldsymbol{\alpha}$ is defined as the stable, proper and inversely stable $m|m$ rational matrix

$$\boldsymbol{\alpha} \stackrel{\Delta}{=} \boldsymbol{\mathcal{R}}\boldsymbol{\mathcal{A}} + \boldsymbol{\mathcal{S}}\boldsymbol{\mathcal{B}} \quad . \tag{3.15}$$

Remark 3.2: The way $\boldsymbol{\mathcal{W}}$ enters $\boldsymbol{\mathcal{H}}_\delta$ in (3.14) is analogous to the way F/P enters $\mathcal{H}_\delta$ in (2.11). Note also that $\boldsymbol{\mathcal{H}}_{nom}(q)$ is unaffected by $\boldsymbol{\mathcal{W}}(q)$, just as in the scalar case (2.10). This means that $\boldsymbol{\mathcal{W}}(q)$ will have a similar effect on the dynamic properties of $\boldsymbol{\mathcal{H}}_\delta$, as P/F has on $\mathcal{H}_\delta$ in (2.11).

Inserting (3.4) into (3.10) gives

$$\begin{aligned} u(k) &= (\mathbf{I} - \boldsymbol{\mathcal{W}}\boldsymbol{\mathcal{R}} - \boldsymbol{\mathcal{W}}\boldsymbol{\mathcal{S}}\boldsymbol{\mathcal{B}}\boldsymbol{\mathcal{A}}^{-1})v(k) + \boldsymbol{\mathcal{W}}\boldsymbol{\mathcal{T}} r(k) \\ &= -(\boldsymbol{\mathcal{W}}(\boldsymbol{\mathcal{R}} + \boldsymbol{\mathcal{S}}\boldsymbol{\mathcal{B}}\boldsymbol{\mathcal{A}}^{-1}) - \mathbf{I})v(k) + \boldsymbol{\mathcal{W}}\boldsymbol{\mathcal{T}} r(k) \\ &= -(\boldsymbol{\mathcal{W}}(\boldsymbol{\mathcal{R}}\boldsymbol{\mathcal{A}} + \boldsymbol{\mathcal{S}}\boldsymbol{\mathcal{B}})\boldsymbol{\mathcal{A}}^{-1} - \mathbf{I})v(k) + \boldsymbol{\mathcal{W}}\boldsymbol{\mathcal{T}} r(k) \end{aligned} \tag{3.16}$$

where the transfer operator

$$\boldsymbol{\mathcal{W}}(\boldsymbol{\mathcal{R}}\boldsymbol{\mathcal{A}} + \boldsymbol{\mathcal{S}}\boldsymbol{\mathcal{B}})\boldsymbol{\mathcal{A}}^{-1} - \mathbf{I}$$

is the multivariable loop gain around the saturations shown in Figure 3.1. This loop gain will be denoted by

$$\begin{aligned} \boldsymbol{\mathcal{L}}_v &\stackrel{\Delta}{=} \boldsymbol{\mathcal{W}}(\boldsymbol{\mathcal{R}}\boldsymbol{\mathcal{A}} + \boldsymbol{\mathcal{S}}\boldsymbol{\mathcal{B}})\boldsymbol{\mathcal{A}}^{-1} - \mathbf{I} \\ &= \boldsymbol{\mathcal{W}}\boldsymbol{\alpha}\boldsymbol{\mathcal{A}}^{-1} - \mathbf{I} \quad . \end{aligned} \tag{3.17}$$

To facilitate the design and make use of the systematic approach developed for scalar control signals, the loop gain $\boldsymbol{\mathcal{L}}_v$ is required to be diagonal, see Figure 3.2. Due to Remark 3.2 and the expression for the loop gain in (3.17), we will chose $\boldsymbol{\mathcal{F}}(q)$ in (3.11) as

$$\boldsymbol{\mathcal{F}}(q) = \boldsymbol{\alpha}(q) \quad . \tag{3.18}$$

As we shall see in Section 3.3, this choice of $\boldsymbol{\mathcal{F}}(q)$ is suitable also for the systematic anti-windup design. The loop gain is then given by

$$\boldsymbol{\mathcal{L}}_v = \boldsymbol{\mathcal{P}}\boldsymbol{\mathcal{A}}^{-1} - \mathbf{I} \quad . \tag{3.19}$$

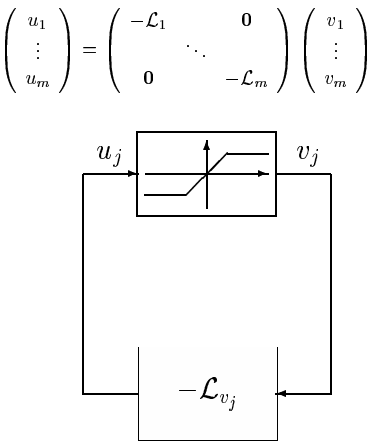

Figure 3.2: The loop gain around the control signal saturation elements, $\boldsymbol{\mathcal{L}}$ is diagonalized by $\boldsymbol{\mathcal{W}}$ into m scalar loop gains $\mathcal{L}_j$. Effects of saturations in different control elements can therefore be analyzed and controlled separately.

The assumption that $\boldsymbol{\mathcal{A}}$ is diagonal will make $\boldsymbol{\mathcal{L}}_v$ become diagonal only if $\boldsymbol{\mathcal{P}}$ is chosen to be diagonal. Consequently,

$$\boxed{\boldsymbol{\mathcal{W}}(q) = \boldsymbol{\mathcal{P}}(q)\boldsymbol{\alpha}^{-1}(q)} \tag{3.20}$$

will be a suitable choice of the anti-windup compensator, introduced in (3.11), if the following requirements are met.

1. $\boldsymbol{\mathcal{P}}(q)$ has to be diagonal in order to obtain a diagonal loop gain $\boldsymbol{\mathcal{L}}_v$.
2. In order to realize the anti-windup compensated controller in (3.10), $\boldsymbol{\mathcal{W}}(q)$ has to be stable. This means that $\boldsymbol{\mathcal{P}}(q)$ has to be chosen stable.
3. To assure stability of $\boldsymbol{\mathcal{W}}$, the factor $\boldsymbol{\alpha}^{-1}$ must be stable. This requirement is already met by the design of the nominal closed loop system.
4. The shape of $\boldsymbol{\mathcal{H}}_\delta(q)$ in (3.14) gives that $\boldsymbol{\mathcal{W}}^{-1}(q)$ has to be chosen stable. This is assured if $\boldsymbol{\mathcal{P}}^{-1}(q)$ is chosen stable. Note that $\boldsymbol{\alpha}(q)$ is stable since $\boldsymbol{\mathcal{R}}$, $\boldsymbol{\mathcal{S}}$, $\boldsymbol{\mathcal{A}}$ and $\boldsymbol{\mathcal{B}}$ all are stable fractional representations.

3.3 Systematic MIMO anti-windup design

The idea is now to adjust the elements of $\boldsymbol{\mathcal{P}}(q)$ in (3.11) by utilizing a criterion which is a direct generalization of (2.14)

$$\begin{aligned} J &= \|\boldsymbol{\mathcal{H}}_\delta\|_2^2 + \left\|\mathbf{Q}\left((\boldsymbol{\mathcal{L}}_v + \mathbf{I})^{-1} - \mathbf{I}\right)\right\|_2^2 \\ &= \left\|\boldsymbol{\mathcal{B}}\boldsymbol{\alpha}^{-1}\boldsymbol{\mathcal{W}}^{-1}\right\|_2^2 + \left\|\mathbf{Q}\left(\boldsymbol{\mathcal{A}}\boldsymbol{\alpha}^{-1}\boldsymbol{\mathcal{W}}^{-1} - \mathbf{I}\right)\right\|_2^2 \quad . \end{aligned} \tag{3.21}$$

The constant diagonal weight matrix

$$\mathbf{Q} = \begin{pmatrix} \sqrt{\rho_1} & & \mathbf{0} \\ & \ddots & \\ \mathbf{0} & & \sqrt{\rho_m} \end{pmatrix} \tag{3.22}$$

is analogous to the square root of the scalar weight parameter ρ in (2.14). By insertion of (3.20) into (3.21), the criterion can be rewritten as

$$J = \left\| \boldsymbol{\mathcal{B}}\boldsymbol{\mathcal{P}}^{-1} \right\|_2^2 + \left\| \mathbf{Q}\left(\boldsymbol{\mathcal{A}}\boldsymbol{\mathcal{P}}^{-1} - \mathbf{I}\right) \right\|_2^2 \tag{3.23}$$

where

$$\mathbf{Q}\left(\boldsymbol{\mathcal{A}}\boldsymbol{\mathcal{P}}^{-1} - \mathbf{I}\right) = \operatorname{diag}\left\{ \sqrt{\rho_j}\left(\frac{\mathcal{A}_j}{\mathcal{P}_j} - 1\right)\right\} \tag{3.24}$$

$$\boldsymbol{\mathcal{B}}\boldsymbol{\mathcal{P}}^{-1} = \left(\frac{\boldsymbol{\mathcal{B}}_1}{\mathcal{P}_1} \quad \dots \frac{\boldsymbol{\mathcal{B}}_m}{\mathcal{P}_m}\right) \tag{3.25}$$

and where $\boldsymbol{\mathcal{B}}_1 \dots \boldsymbol{\mathcal{B}}_m$ are the columns of $\boldsymbol{\mathcal{B}}$. Now, (3.24) and (3.25) allows us to express (3.23), using *Parsevals formula*, as

$$\begin{aligned}
J &= \left\| \left(\frac{\boldsymbol{\mathcal{B}}_1}{\mathcal{P}_1} \quad \frac{\boldsymbol{\mathcal{B}}_2}{\mathcal{P}_2} \dots \frac{\boldsymbol{\mathcal{B}}_m}{\mathcal{P}_m}\right) \right\|_2^2 + \left\| \operatorname{diag}\left\{ \sqrt{\rho_j}\left(\frac{\mathcal{A}_j}{\mathcal{P}_j} - 1\right)\right\} \right\|_2^2 \\
&= \frac{1}{2\pi}\oint_{|z|=1} \operatorname{tr}\left\{ \left(\frac{\boldsymbol{\mathcal{B}}_1}{\mathcal{P}_1} \quad \frac{\boldsymbol{\mathcal{B}}_2}{\mathcal{P}_2} \dots \frac{\boldsymbol{\mathcal{B}}_m}{\mathcal{P}_m}\right)\left(\frac{\boldsymbol{\mathcal{B}}_1}{\mathcal{P}_1} \quad \frac{\boldsymbol{\mathcal{B}}_2}{\mathcal{P}_2} \dots \frac{\boldsymbol{\mathcal{B}}_m}{\mathcal{P}_m}\right)^* \right\} \frac{dz}{z} \\
&+ \frac{1}{2\pi}\oint_{|z|=1} \operatorname{tr}\left\{ \left(\operatorname{diag}\left\{ \sqrt{\rho_j}\left(\frac{\mathcal{A}_j}{\mathcal{P}_j} - 1\right)\right\}\right)\left(\operatorname{diag}\left\{ \sqrt{\rho_j}\left(\frac{\mathcal{A}_j}{\mathcal{P}_j} - 1\right)\right\}\right)^* \right\} \frac{dz}{z} \\
&= \frac{1}{2\pi}\oint_{|z|=1} \operatorname{tr}\left\{ \frac{\boldsymbol{\mathcal{B}}_1\boldsymbol{\mathcal{B}}_1^*}{\mathcal{P}_1\mathcal{P}_1^*} + \frac{\boldsymbol{\mathcal{B}}_2\boldsymbol{\mathcal{B}}_2^*}{\mathcal{P}_2\mathcal{P}_2^*} + \dots + \frac{\boldsymbol{\mathcal{B}}_m\boldsymbol{\mathcal{B}}_m^*}{\mathcal{P}_m\mathcal{P}_m^*} \right\} \frac{dz}{z} \\
&+ \frac{1}{2\pi}\oint_{|z|=1} \operatorname{tr}\left\{ \operatorname{diag}\left\{ \rho_j \left(\frac{\mathcal{A}_j}{\mathcal{P}_j} - 1\right)\left(\frac{\mathcal{A}_j}{\mathcal{P}_j} - 1\right)^* \right\} \right\} \frac{dz}{z} \quad .
\end{aligned} \tag{3.26}$$

It is obvious that the expression (3.26) can be decomposed into a sum of m separate pairs of integrals

$$J = \sum_{j=1}^{m} \frac{1}{2\pi}\oint_{|z|=1} \frac{\operatorname{tr}\left\{\boldsymbol{\mathcal{B}}_j\boldsymbol{\mathcal{B}}_j^*\right\}}{\mathcal{P}_j\mathcal{P}_j^*}\frac{dz}{z} + \frac{1}{2\pi}\oint_{|z|=1} \rho_j \left(\frac{\mathcal{A}_j}{\mathcal{P}_j} - 1\right)\left(\frac{\mathcal{A}_j}{\mathcal{P}_j} - 1\right)^* \frac{dz}{z} \tag{3.27}$$

Each term of the sum is influenced by a separate ρ_j and a separate $\mathcal{P}_j$ for $j = 1, 2 \ldots m$. Thus, the criterion (3.23) can be rewritten as a sum of m quadratic criteria which may be minimized separately with respect to $\mathcal{P}_j$, i.e.

$$J = \sum_{j=1}^{m} J_j \quad , \tag{3.28}$$

where J_j is given by

$$J_j = \frac{1}{2\pi} \oint_{|z|=1} \frac{\sum_{i=1}^{p} \mathcal{B}_{ij}\mathcal{B}_{ij}^*}{\mathcal{P}_j\mathcal{P}_j^*} \frac{dz}{z} + \frac{1}{2\pi} \oint_{|z|=1} \rho_j \left(\frac{\mathcal{A}_j}{\mathcal{P}_j} - 1\right) \left(\frac{\mathcal{A}_j}{\mathcal{P}_j} - 1\right)^* \frac{dz}{z} \quad . \tag{3.29}$$

In (3.29) we used that the numerator inside the first integral in (3.27) can be expressed as

$$\mathrm{tr}\{\boldsymbol{\mathcal{B}}_j\boldsymbol{\mathcal{B}}_j^*\} = \sum_{i=1}^{p} \mathcal{B}_{ij}\mathcal{B}_{ij}^* \tag{3.30}$$

where p is the number of process outputs and $\mathcal{B}_{ij}$ is the ijth element of $\boldsymbol{\mathcal{B}}$.

Minimizing (3.28) will thus be the same as minimizing m separate criteria, each of which will be minimized by solving a spectral factorization of the type (2.16). Minimizing (3.23) with respect of the elements of $\boldsymbol{\mathcal{P}}$ for a given matrix $\mathbf{Q}$, will consequently require m scalar spectral factorizations. The optimal choice of the stable transfer operator $\mathcal{P}_j(q)$ is then obtained from the scalar rational spectral factorization equation,

$$\boxed{r\mathcal{P}_j\mathcal{P}_j^* = \sum_{i=1}^{p} \mathcal{B}_{ij}\mathcal{B}_{ij}^* + \rho_j\mathcal{A}_j\mathcal{A}_j^*} \tag{3.31}$$

which has to be solved for $j = 1, 2 \ldots . m$, where m is the number of process inputs. If the stable denominator polynomial of $\mathcal{P}_j\mathcal{P}_j^*$ (left-hand side of (3.31)) is chosen as the known stable denominator polynomial of the right-hand side of (3.31), then (3.31) can be solved as a scalar polynomial spectral factorization equation. This completes the design of the anti-windup compensator $\boldsymbol{\mathcal{W}}$ in (3.11), (3.20) for a given set of scalar penalties ρ_j. The transfer function $\boldsymbol{\mathcal{H}}_\delta$, for desaturation transients, will be given by (3.25), see Figure 3.3 and the matrix (3.17) representing the loop gains around the control signal saturations, is given by

$$\boldsymbol{\mathcal{L}}_v \;=\; \boldsymbol{\mathcal{P}}\boldsymbol{\mathcal{A}}^{-1} - \mathbf{I} \;=\; \mathrm{diag}\left(\frac{\mathcal{P}_j}{\mathcal{A}_j} - 1\right) \quad . \tag{3.32}$$

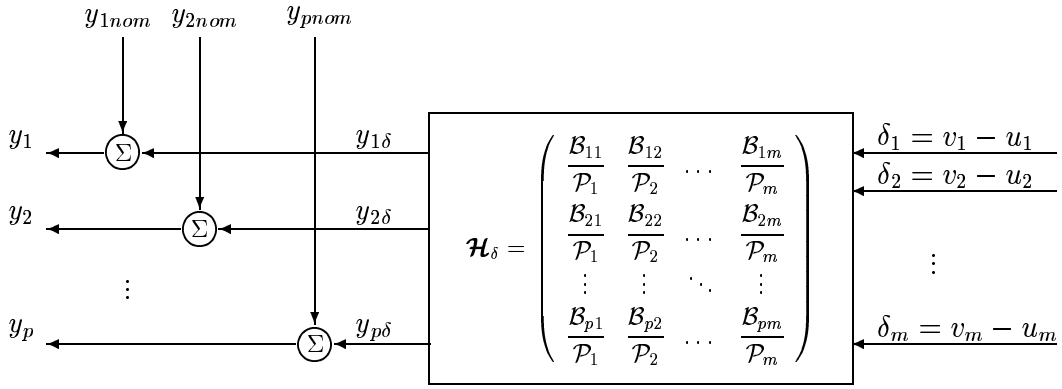

Figure 3.3: The resulting linear dynamics of the desaturation transients. The stabel transfer operator $\mathcal{P}_j$ occurs as a common denominator of each element in column j of $\boldsymbol{\mathcal{H}}_\delta$ and hence, the "pertubation" $y_{i\delta_j}$, $i = 1 \dots p$, caused by desaturation in the jth loop, can be given desired dynamic properties by an appropriate choice of $\mathcal{P}_j$.

An intuitive explainition of why (3.31) will give the optimal choice of $\mathcal{P}_j$, in the sense of minimizing the effect of a saturation event as seen from the process outputs, as (2.16) gave in the scalar case, is given next.

If we are interested in the design of an anti-windup compensator around the jth actuator, by considering the dynamic properties of $\boldsymbol{\mathcal{H}}_\delta$, then the only components of $u(k)$ and $v(k)$ involved in such a design procedure will be $u_j(k)$ and $v_j(k)$. See Figure 3.3. Consequently, if only the jth actuator saturates then the pertubation $y_\delta = \boldsymbol{\mathcal{H}}_\delta \delta$ will only be affected by δ_j. This means that the dynamics excited by a saturation event in the jth loop, i.e. a saturation in the jth actuator, will be described exclusively by the jth *column* of $\boldsymbol{\mathcal{H}}_\delta$. In Chapter 2 we discussed the trade-off between minimizing $\mathcal{H}_\delta$ and keeping the loop gain away from the NLCF. In analogy with that discussion, there is now a trade-off between minimizing the jth column of $\boldsymbol{\mathcal{H}}_\delta$ and and keeping the jth loop gain away from the jth NLCF, see Figure 3.4. An appropriate compromise choice of the scalar anti-windup filter $\mathcal{P}_j$ in such a case, is then obtained by solving the spectral factorization (3.31).

Note that the scalar ρ_j in (3.31) has a similar effect on the design of $\mathcal{P}_j$, as the weighting ρ in (2.16) has on the design of P in the scalar case, see Figure 3.4.

Let us look at a typical design example by assuming that we have diagonalized the loop gain around the saturations, so that m scalar loop gains is to be adjusted in relation to the m NonLinearity Characteristic Functions (NLCFs). The situation is illustrated in Figure 3.5. As we can see, the second loop gain $\mathcal{L}_{v_2}$ intresects the $NLCF_2$, which may cause repeated re-saturations and/or limit cycle oscillations in that loop. If this is the case, it will, of course, have a negativ affect on the whole system. To avoid the possible occurrence of such undesired affects, the loop gain $\mathcal{L}_{v_2}$ has to be decreased. An opposite situation is present in the mth

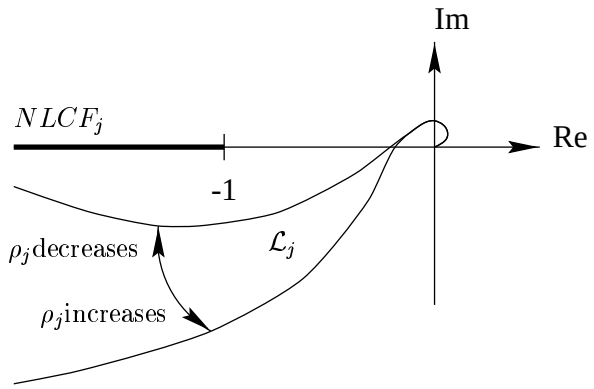

Figure 3.4: The jth loop gain $\mathcal{L}_j$. The distance from the $NLCF_j$ is controlled by increasing or decreasing ρ_j.

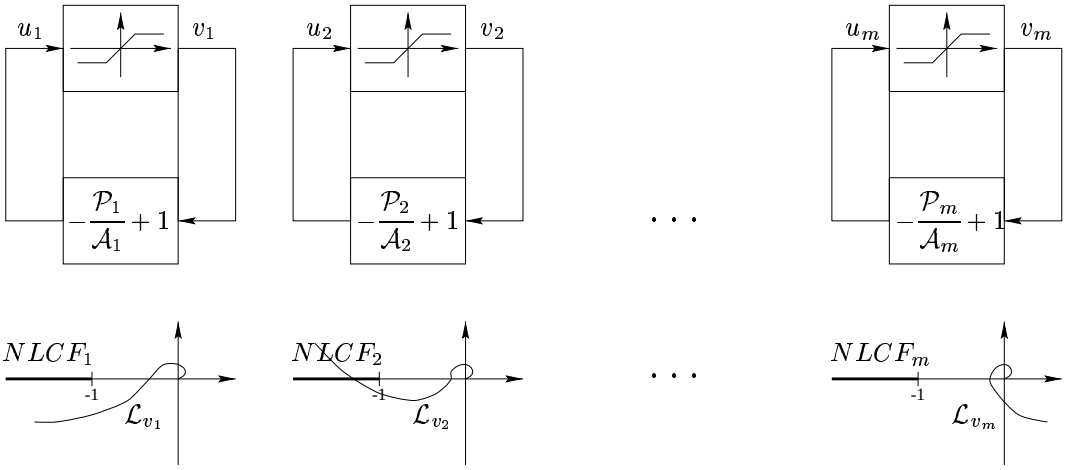

Figure 3.5: The m scalar loop gains around the m, possibly saturating, actuators. Each loop gain $\mathcal{L}_{v_j} = (\mathcal{P}_j/\mathcal{A}_j - 1)$ can be adjusted by an appropriate choice of $\mathcal{P}_j$.

loop. The mth loop gain may be increased, i.e. it may be possible to "blow up" $\mathcal{L}_{v_m}$, in order to obtain a faster desaturation transient, without obtaining repeated-resaturations and/or limit cycle oscillations. The loop gain $\mathcal{L}_{v_1}$ seems to have an appropriate location already.[2]

When the adjustments proposed above are made, we must simulate the system to see how it performs. A step response of the desaturation-transient dynamics, $\boldsymbol{\mathcal{H}}_\delta$, will enlighten us of how further adjustments are to be made, as well.

[2]This discussion is true in general but, since different plants and actuators have different dynamic properties, one sufficiently relative location between a NLCF and its correspondig loop gain, may not be sufficient for another loop gain-NLCF configuration.

Chapter 4

Anti-Windup Compensators for Decoupled MIMO Systems

The method of feedforward decoupling is frequently used in practical control applications. The reason for this is that conventional PID controllers, which are the most common controllers in industrial applications, can only be used in single loops, i.e. in SISO systems. Nevertheless, such control systems will, of course, suffer from control signal saturation. Therefore, we will in this chapter suggest an anti-windup compensation strategie specially adapted to feedforward-decoupled systems. The method is based on the systematic anti-windup concept discussed in the previous chapters. The resulting design is simpler than the one discussed in Chapter 3, in the sense that it involves the adjustment of only one scalar loop gain, which requires only a single spectral factorization.

Dynamic-feedforward decoupling of processes with m inputs and p outputs is first discussed in Section 4.1. Thereafter our discussions consider only square MIMO processes.

A method for the design of a feedforward-decoupling controller will also be discussed. This decoupling controller consists of a set of scalar polynomial controllers, on RST-form (2.2), in conjuction with a decoupling link.

Readers who intend to append anti-windup compensation to PID controllers which work in conjunction with a decoupling link should note that all design methods discussed in this report, assume knowledge of a plant model. While there is normally some kind of plant model available from the design of the decoupling link, this model may not be sufficiently accurate for the design of the anti-windup compensator.

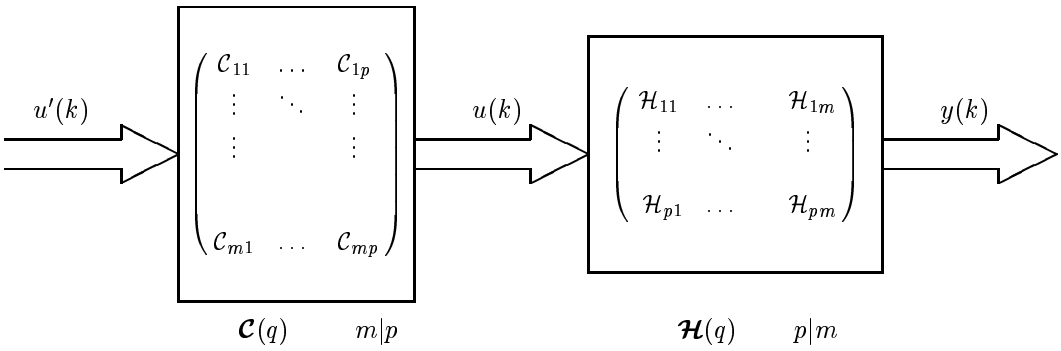

Figure 4.1: A feedforward decoupling compensator $\boldsymbol{\mathcal{C}}(q)$ in series with the system $\boldsymbol{\mathcal{H}}(q)$ with m inputs and p outputs. Here, $m \geq p$ is required.

4.1 Feedforward decoupling compensation

Two drawbacks of decoupling must be stated from the beginning. First, a dynamic feedforward decoupling link will tend to consist of transfer functions of high order. Second, some of the resulting control signals may have large amplitudes, in particular if the plant is ill-conditioned. Therefore, decoupling is not always the best approach to the design of a well performing multivariable controller. This is true in particular if the process is of high order.[1]

The saturation nonlinearity of the system will be neglected at this stage, which means that we will treat the system as if it were linear. The nonlinearity is taken into account in Section 4.2.2.

Let the MIMO process with m inputs and p outputs, with $m \geq p$, be decribed by

$$y(k) = \boldsymbol{\mathcal{H}}(q)u(k) \quad , \tag{4.1}$$

where $\boldsymbol{\mathcal{H}}(q)$ is assumed to be stable or marginally stable. Then, by connecting a stable $p|m$ matrix transfer operator $\boldsymbol{\mathcal{C}}(q)$ to the input of the process $\boldsymbol{\mathcal{H}}(q)$, it is sometimes possible to obtain a decoupled system $\boldsymbol{\mathcal{D}}(q)$. Let $u'(k)$ denote the input signals to $\boldsymbol{\mathcal{D}}(q)$. The signal vectors $u(k)$ and $u'(k)$ are then related by

$$u(k) = \boldsymbol{\mathcal{C}}(q)u'(k) \quad . \tag{4.2}$$

Total decoupling is obtained if $\boldsymbol{\mathcal{H}}(q)\boldsymbol{\mathcal{C}}(q)$ is diagonal, that is, if

$$\boldsymbol{\mathcal{H}}(q)\boldsymbol{\mathcal{C}}(q) = \boldsymbol{\mathcal{D}}(q) = \begin{pmatrix} \mathcal{D}_1(q) & & \mathbf{0} \\ & \ddots & \\ \mathbf{0} & & \mathcal{D}_p(q) \end{pmatrix} \tag{4.3}$$

[1] It is not always necassary to use a dynamic decoupling link. If we can accept weak cross couplings, a static decoupling link will in many cases be sufficient. However, we will only concider dynamic decoupling links in this report.

where the matrix $\boldsymbol{\mathcal{D}}$ is of dimension $p|p$. The decoupled system consists of p mutually independent SISO systems instead of a MIMO system containing cross couplings. See Figure 4.1. With a few exceptions, each one of these SISO systems can then be handeled by conventional SISO controller design.[2] For similar reasons as those discussed in Chapter 2, concerning stability whenever the control signal saturates, we will require that all of the scalar transfer operators $\mathcal{D}_i(q)$ are stable or marginally stable and, of course, also proper.

The feedforward decoupling compensator $\boldsymbol{\mathcal{C}}(q)$ is then given by

$$\boldsymbol{\mathcal{C}}(q) = \boldsymbol{\mathcal{H}}^{-1}(q)\boldsymbol{\mathcal{D}}(q) \tag{4.4}$$

where all elements of $\boldsymbol{\mathcal{C}}(q)$ must, for the same reasons as above, be stable and proper.

If some modes of $\boldsymbol{\mathcal{H}}^{-1}(q)$ are unstable, we have to select some of the transfer operators $\mathcal{D}_i(q)$ in such a way that they cancel out these unstable modes. Thus, $\mathcal{D}_i(q)$ may be required to have zeros outside of the unit circle. This might complicate the design of a suitable feedback.[3] Such cancellations must, of course, be made before the decoupling compensator $\boldsymbol{\mathcal{C}}(q)$ is implemented.

4.2 Decoupling and control of square systems

In the case of square systems, it is possible to select a special solution to find suitable compensators $\boldsymbol{\mathcal{C}}(q)$ and a resulting diagonalized system $\boldsymbol{\mathcal{D}}(q)$. If $\boldsymbol{\mathcal{H}}(q)$, of dimension $(p|p)$, is the system considered, then $\boldsymbol{\mathcal{H}}^{-1}(q)$ can be expressed as

$$\boldsymbol{\mathcal{H}}^{-1}(q) = \frac{\mathrm{Adj}(\boldsymbol{\mathcal{H}}(q))}{\det(\boldsymbol{\mathcal{H}}(q))} \tag{4.5}$$

so that

$$\boldsymbol{\mathcal{C}} = \boldsymbol{\mathcal{H}}^{-1}\boldsymbol{\mathcal{D}} = \frac{\mathrm{Adj}(\boldsymbol{\mathcal{H}})}{\det(\boldsymbol{\mathcal{H}})}\boldsymbol{\mathcal{D}} \quad . \tag{4.6}$$

Since all elements of $\boldsymbol{\mathcal{H}}(q)$ are assumed to be stable, or marginally stable, and proper, all elements of $\mathrm{Adj}(\boldsymbol{\mathcal{H}})$ are stable, or marginally stable, and proper and so is $\det(\boldsymbol{\mathcal{H}})$. In agreement with what was said before, $\det(\boldsymbol{\mathcal{H}})$ probably has some zeros outside the unit circle, which makes $1/\det(\boldsymbol{\mathcal{H}})$ unstable.

[2] One of these exceptions becomes obvious in LQ controller design. A penalty on the input signal to $\boldsymbol{\mathcal{C}}(q)$, does not have the same effect as a penalty on the real controller output signal $u(k)$.

[3] This is, of course, not an unexpected effect. The zeros of $\boldsymbol{\mathcal{H}}(q)$ which lie outside the region of stability, are also those which make $\boldsymbol{\mathcal{H}}^{-1}(q)$ unstable. Such zeros can never be canceled without obtaining hidden unstable modes in the controller.

One possible, and suitable, choice of $\boldsymbol{\mathcal{D}}(q)$ would then be

$$\boldsymbol{\mathcal{D}}(q) = \det(\boldsymbol{\mathcal{H}}(q))\mathbf{I}_p \tag{4.7}$$

and hence (4.6) and (4.7) give

$$\boldsymbol{\mathcal{C}}(q) = \mathrm{Adj}(\boldsymbol{\mathcal{H}}(q)) \quad . \tag{4.8}$$

The MIMO system $\boldsymbol{\mathcal{H}}(q)$ has thus been diagonalized into n SISO-systems, all with the transfer function $\det(\boldsymbol{\mathcal{H}}(q))$. Note that some transmission poles and transmissions zero might cancel each other in the realization of $\det(\boldsymbol{\mathcal{H}}(q))$ [10]. We will, in the following, assume that there exists no common marginally stable factors in $\det(\boldsymbol{\mathcal{H}}(q))$.

4.2.1 Controller design

Due to the fact that all the p decoupled systems have the same dynamics, only *one* SISO controller design has to be performed. This can, for instance, be done with the LQG methods suggested in [11], yielding the controller

$$R'u_i'(k) = -S'y_i(k) + T'r_i(k) \tag{4.9}$$

where the index i denotes the ith components of the control signal $u'(k)$, the measured plant-output signal $y(k)$ and the reference signal vector $r(k)$ respectively.

These n SISO controllers correspond to one MIMO controller of the system

$$\begin{aligned} y(k) &= \boldsymbol{\mathcal{D}}u'(k) \\ \boldsymbol{R}'u'(k) &= -\boldsymbol{S}'y(k) + \boldsymbol{T}'r(k) \end{aligned} \tag{4.10}$$

where

$$\begin{aligned} \boldsymbol{R}'(q) &= R'(q)\mathbf{I}_p & (4.11)\\ \boldsymbol{S}'(q) &= S'(q)\mathbf{I}_p & (4.12)\\ \boldsymbol{T}'(q) &= T'(q)\mathbf{I}_p \quad . & (4.13) \end{aligned}$$

According to (4.2) and (4.10)-(4.13), the total multivariable controller is obtained as

$$\boldsymbol{R}u(k) = -\boldsymbol{\mathcal{S}}y(k) + \boldsymbol{\mathcal{T}}r(k) \tag{4.14}$$

where

$$\boldsymbol{R}(q) = \boldsymbol{R}'(q) = R'(q)\mathbf{I}_p \tag{4.15}$$
$$\boldsymbol{\mathcal{S}}(q) = \boldsymbol{\mathcal{C}}(q)\boldsymbol{S}'(q) = \mathrm{Adj}(\boldsymbol{\mathcal{H}}(q))S'(q) \tag{4.16}$$
$$\boldsymbol{\mathcal{T}}(q) = \boldsymbol{\mathcal{C}}(q)\boldsymbol{T}'(q) = \mathrm{Adj}(\boldsymbol{\mathcal{H}}(q))T'(q) \quad . \tag{4.17}$$

Notice that the feedforward decoupling link $\boldsymbol{\mathcal{C}}(q)$ is included in the structure of the nominal polynomial matrix controller (4.14).

The next step is to take constraints on the control signal into account. With a decoupled closed loop system, it will be straightforward to obtain a diagonal loop gain matrix, which can be used together with Nyquist-like methods as before. A transfer operator matrix $\boldsymbol{\mathcal{W}}(q)$ can then be appended to the nominal controller (4.10), to control the saturation properties.

4.2.2 Loop gains around the saturations and AWC

The system has a configuration described by Figure 3.1. Recall that $u(k)$ is the actual input signal to the process and hence this signal will suffer from saturation, not $u'(k)$.

By utilizing the anti-windup controller (3.10) with $\boldsymbol{\mathcal{R}}$, $\boldsymbol{\mathcal{S}}$ and $\boldsymbol{\mathcal{T}}$ given by (4.15)-(4.17), the loop gain (3.17) around the saturations becomes

$$\boldsymbol{\mathcal{L}}_v = \boldsymbol{\mathcal{W}}(\boldsymbol{R} + \boldsymbol{\mathcal{S}}\boldsymbol{\mathcal{H}}) - \mathbf{I}_p \tag{4.18}$$

where

$$\boldsymbol{\mathcal{S}}\boldsymbol{\mathcal{H}} = S'\boldsymbol{\mathcal{C}}\boldsymbol{\mathcal{H}} = S'\boldsymbol{\mathcal{D}} = S'\det(\boldsymbol{\mathcal{H}})\mathbf{I}_p \quad . \tag{4.19}$$

Note that $\boldsymbol{\mathcal{S}}\boldsymbol{\mathcal{H}}$ is a scalar transfer operator times a unit matrix of dimension $p|p$. By rewriting $\det(\boldsymbol{\mathcal{H}})$ as a polynomial ratio

$$\frac{B_{det}(q)}{A_{det}(q)} \triangleq \det(\boldsymbol{\mathcal{H}}(q)) \tag{4.20}$$

and combining this ratio with (4.19) and (4.18), the loop gain $\boldsymbol{\mathcal{L}}_v$ can be written as

$$\boldsymbol{\mathcal{L}}_v = \boldsymbol{\mathcal{W}}(R'A_{det} + S'B_{det})\frac{1}{A_{det}} - \mathbf{I}_p \quad . \tag{4.21}$$

If $\boldsymbol{\mathcal{W}}$ in (4.21) is chosen to be a scalar transfer operator times the unit matrix $\mathbf{I}_p$, i.e.

$$\boldsymbol{\mathcal{W}}(q) = \frac{P(q)}{F(q)}\mathbf{I}_p \quad , \tag{4.22}$$

then the rational matrix expression of the loop gain, $\boldsymbol{\mathcal{L}}_v$, simply becomes a scalar transfer operator times a unit matrix of dimension $p|p$. This is the choice of $\boldsymbol{\mathcal{W}}$ that we will use from now on. The final scalar expression for each one of these loop gains is, in such a case

$$\mathcal{L}_v \;=\; \frac{P(R'A_{det} + S'B_{det})}{FA_{det}} - 1 \quad . \tag{4.23}$$

Note that (4.23) is analogous to (2.13). Before we can formulate a suitable anti-windup design procedure, which will help us to find suitable polynomials F and P, we need to know how F and P will influence the dynamic properties of $\boldsymbol{\mathcal{H}}_\delta$.

By making use of (3.4), (3.14) and (4.15)-(4.17) we obtain

$$\begin{aligned} \boldsymbol{\mathcal{H}}_\delta \;&=\; \boldsymbol{\mathcal{B}\alpha}^{-1}\boldsymbol{\mathcal{W}}^{-1} \;=\; \boldsymbol{\mathcal{B}\mathcal{A}}^{-1}(\boldsymbol{\mathcal{R}} + \boldsymbol{\mathcal{S}\mathcal{B}\mathcal{A}}^{-1})^{-1}\boldsymbol{\mathcal{W}}^{-1} && (4.24)\\ &=\; \boldsymbol{\mathcal{H}}(\boldsymbol{\mathcal{R}} + \boldsymbol{\mathcal{S}\mathcal{H}})^{-1}\boldsymbol{\mathcal{W}}^{-1} \quad . && (4.25) \end{aligned}$$

Inserting (4.15), (4.19), (4.20) and (4.22) into (4.25) gives the expression

$$\boldsymbol{\mathcal{H}}_\delta \;=\; \boldsymbol{\mathcal{H}}\frac{A_{det}F}{(R'A_{det} + S'B_{det})P} \quad . \tag{4.26}$$

As we can see, the anti-windup polynomials F and P in (4.22) enters $\boldsymbol{\mathcal{H}}_\delta$ in (4.26) in the same way as F and P in (2.5) enters $\mathcal{H}_\delta$ in (2.11).

The choice $F = R'A_{det} + S'B_{det}$, allows us to adjust the loop gains $\mathcal{L}_v$ in (4.23), by an appropriate choice of P in the same way as in Chapter 2.

But, regarding the dynamic properties of $\boldsymbol{\mathcal{H}}_\delta$ in (4.26) , i.e. the dynamic properties of the desaturation transients, this choice of F may leave some of the plant poles left in the exression of $\boldsymbol{\mathcal{H}}_\delta$. If all the transmission poles of $\boldsymbol{\mathcal{H}}$ are factors of A_{det}, then there will be no poles left in $\boldsymbol{\mathcal{H}}_\delta$, except for those given by P. Nevertheless, we will chose the anti-windup polynomial F as

$$\boxed{F = R'A_{det} + S'B_{det}} \tag{4.27}$$

For the design of P, we will use the modified spectral factorization equation

$$\boxed{rPP^* \;=\; B_{det}B^*_{det} + \rho A_{det}A^*_{det}} \quad . \tag{4.28}$$

The 2-norm of $\boldsymbol{\mathcal{H}}_\delta$ is not minimized by the choice $P = B^{stable}_{det}$ and due to this fact, a polynomial P obtained from (4.28) will not minimize a criterion analogous to

(2.14). Still, it will be possible to adjust the loop gains in relation to the NLCFs, by using P, obtained by solving (4.28) for different values of ρ. If the value of ρ is increasing, the polynomial P will approach the stable, or marginally stable polynomial A_{det}. Such a P will force the loop gain curve away from the NLCF and for large values of ρ, the loop gain $\mathcal{L}_v$ will end up as a point in the origin. If the value of ρ is decreasing, the polynomial P will approach the stable, or marginally stable polynomial B_{det}^{stable}. This, in turn, will increase the loop gain $\mathcal{L}_v$ and force it to approach the NLCF.

4.3 Examples

The anti-windup strategy introduced in this chapter will be compared with three other strategies. The nominal controller is a LQ controller designed by the methods discussed earlier in this chapter.

First, we will investigate how the nominal controller performes without anti-windup compensation. Then we will use a method similar to the observer based method by Åström and Wittenmark [1] and also a method similar to the conditioning technique by Hanus, *et.al.* [2]. As a final example, we will investigate how our stategy performs.

The process to be controlled is a *Heavy Oil Fractionator* (HOF), which is used to separate components from crude oil. The HOF has two inputs and two outputs and a plot of the open-loop step responses of the process is shown in Figure 4.2. In all examples, a symmetric nonlinearity with saturation limits $v_{min} = -0.5$ and $v_{max} = 0.5$ will be used.

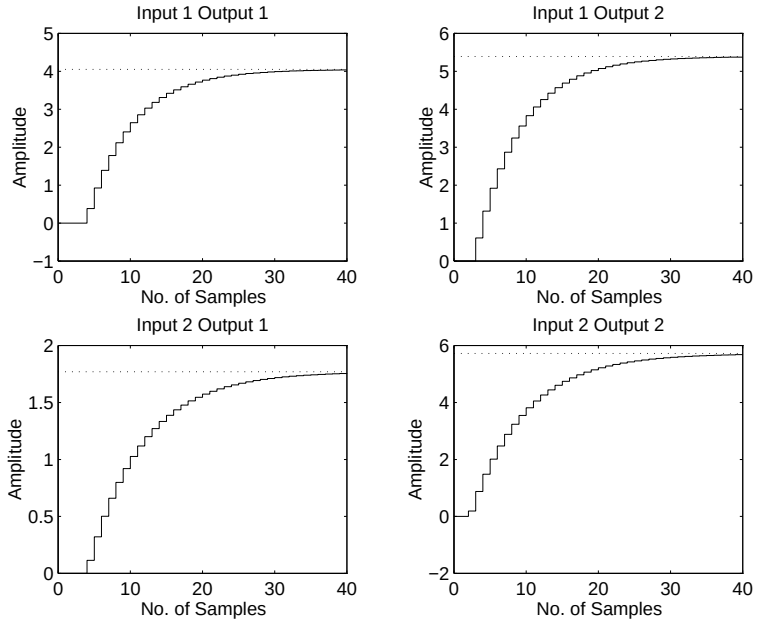

Figure 4.2: Step responses of the Heavy Oil Fractionator process. This HOF is used to separate components from crude oil and the process has two inputs and two outputs. The input $u1$ is a Top Draw of one of these components and the input $u2$ is a Side Draw of another component. Both Draws must be within hard maximum and minimum bounds of $+0.5$ and -0.5. The outputs $y1$ and $y2$ are temperatures at the Top End Point and the Side End Point of the HOF, respectively.

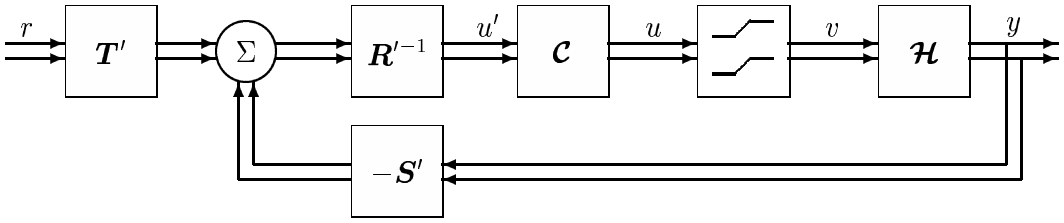

Figure 4.3: Feedforward-decoupling controller, without anti-windup compensation, in conjuction with a process plant $\boldsymbol{\mathcal{H}}$.

Example 1

This first example shows how the system reacts on saturation events when the controller lacks windup compensation. The control law, given by (4.14), is

$$\boldsymbol{R}u = -\boldsymbol{\mathcal{S}}y + \boldsymbol{\mathcal{T}}r \tag{4.29}$$

but, we will realize the controller as

$$\boldsymbol{R}'u = \boldsymbol{\mathcal{C}}(-\boldsymbol{S}'y + \boldsymbol{T}'r) \quad . \tag{4.30}$$

The system is shown in Figure 4.3. This is a LQ-controller designed by use of the method described earlier in this chapter. The decoupling link is thus given by (4.8). For the design of the regulator $\{\boldsymbol{R}', \boldsymbol{S}', \boldsymbol{T}'\}$, the LQ-design criterion

$$J = y^2 + 1.5 * u'^2 \tag{4.31}$$

was used. Here, u' is the input signal vector to the decoupled system $\boldsymbol{\mathcal{D}} = \boldsymbol{\mathcal{H}}\boldsymbol{\mathcal{C}}$. The regulator has one observer pole at $z = 0.75$ and, to obtain integral action, the polynomial R' has one zero in $z = 1$. Futhermore, the scalar polynomial T' is chosen such that $\deg[T'] = \deg[R']$.

Evaluation of the simulation

We note that the loop gain curve not intersects the NLCF (see the bottom diagrams of Figure 4.4), which means that stable cycles should not occur. In the plot of the output signals (top diagrams of Figure 4.4) we observe that such stable cycles are not present. It would, however, be desireble to get rid of the peaks in the output signals, which are caused by the saturation events. One can clearly see how the control signals overshoot there allowed range when the output transients occur (middle diagrams of Figure 4.4).

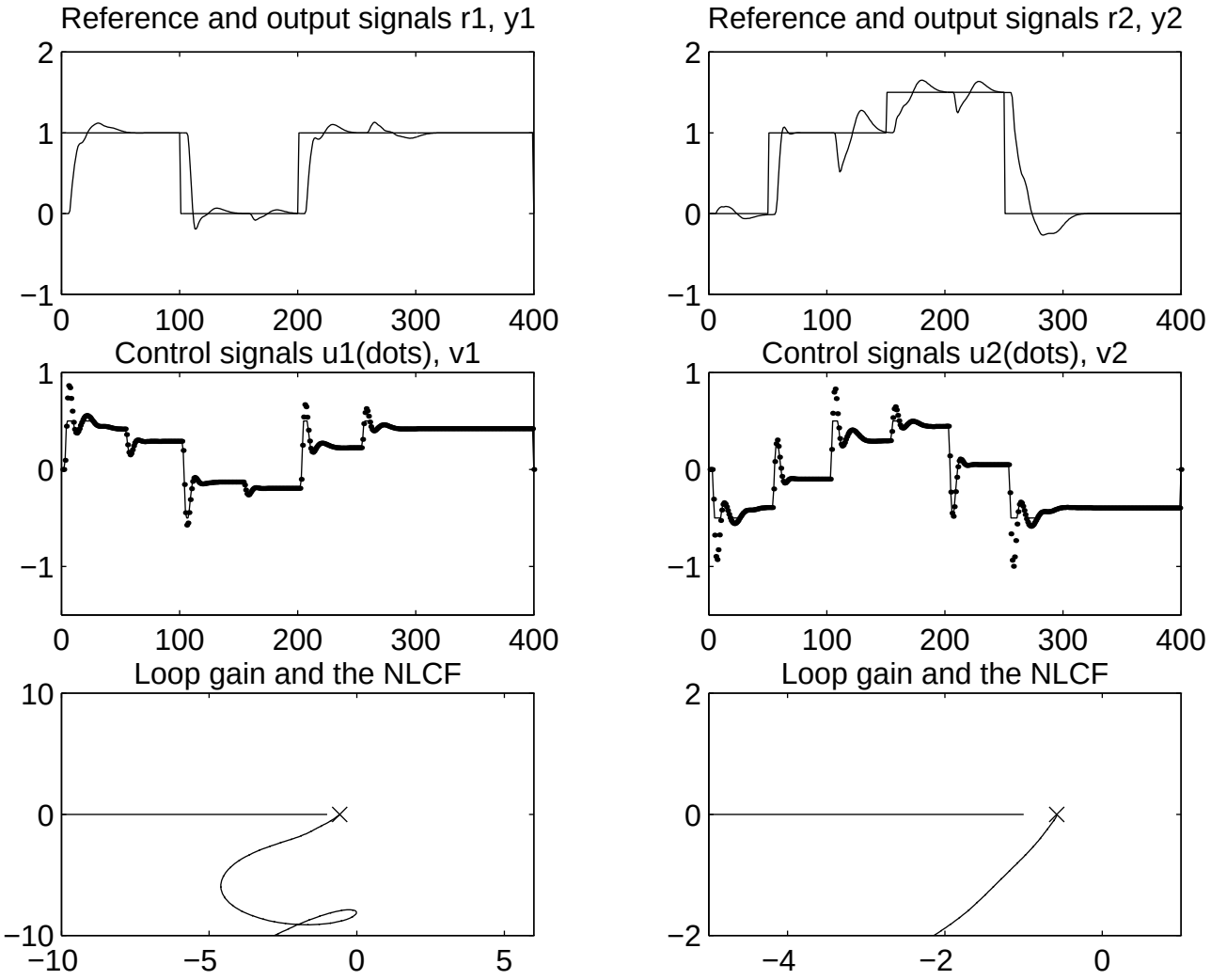

Figure 4.4: The Heavy Oil Fractionator controlled by feedforward-decoupling and two identical LQ controllers, without anti-windup compensation. Since the two loop gains around the two saturating control signal elements are, by design, the same, the two bottom diagrams shows the same loop gain and the same NLCF. The right-bottom diagram is just a magnification of the left-bottom diagram, in the region around the point -1. The reference signals $r1, r2$ and the plant output signals $y1, y2$ are shown in the upper diagrams. The controller output signals $u1, u2$ and the plant input signals $v1, v2$ are shown in the middle diagrams.

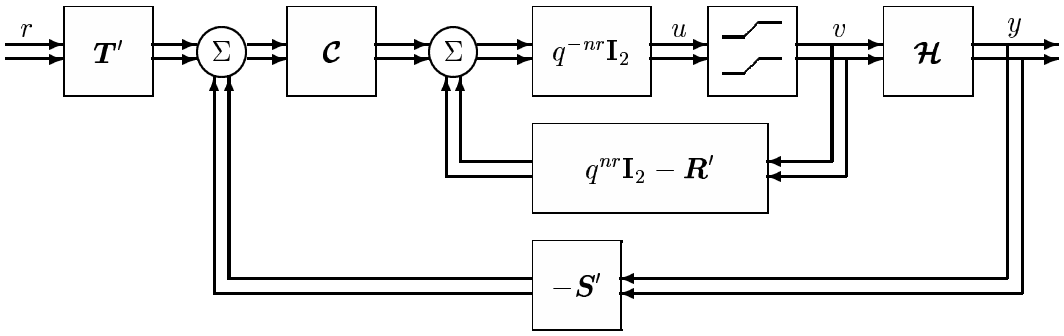

Figure 4.5: Feedforward-decoupling controller, with dead beat anti-windup compensation, in conjuction with a process plant $\boldsymbol{\mathcal{H}}$.

Example 2

The anti-windup compensator used in this example is similar to the deadbeat-observer based anti-windup compensator suggested in [1] for scalar systems. The control law is given by

$$q^{nr}u = (q^{nr}\mathbf{I}_2 - \boldsymbol{R}')v + \boldsymbol{\mathcal{C}}(-\boldsymbol{S}'y + \boldsymbol{T}'r) \quad . \tag{4.32}$$

Figure 4.5 depicts the system. The controller (4.32) can also be seen as a special case of the more general anti-windup compensated control law

$$u = (\mathbf{I}_2 - \boldsymbol{\mathcal{W}}\boldsymbol{R})v - \boldsymbol{\mathcal{W}}\boldsymbol{\mathcal{S}}y + \boldsymbol{\mathcal{W}}\boldsymbol{\mathcal{T}}r \quad . \tag{4.33}$$

These two controllers becomes equal by the choice $\boldsymbol{\mathcal{W}} = q^{-nr}\mathbf{I}_2$.

Evaluation of the simulation

The pre-existing controller, $\{\boldsymbol{R}', \boldsymbol{S}', \boldsymbol{T}'\}$, and the decoupling link $\boldsymbol{\mathcal{C}}$ are the same as in Example 1.

In this case the loop gain curve does intersect the NLCF and, as we can see, the intersection point is located close to the point -1 (bottom diagarams of Figure 4.6). As a consequence, stable cycle oscillations will most likely occur in this system. The behavior of the plant output signals and the controller output signals tells as that this is the case (top and middle diagrams of Figure 4.6). The fact is that the uncompensated controller in Example 1 performed better.

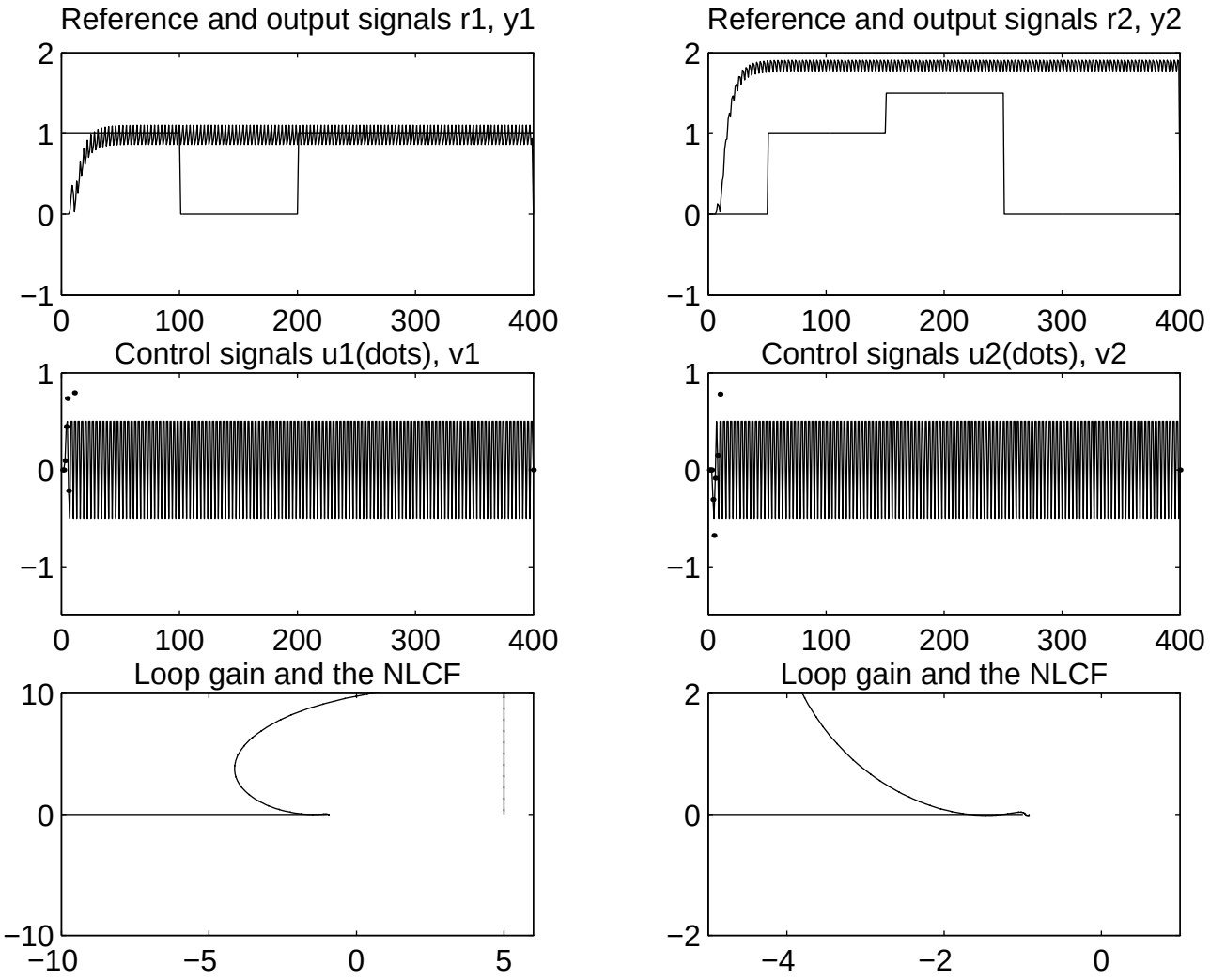

Figure 4.6: The Heavy Oil Fractionator controlled by a feedforward decoupling LQ controller equiped with a deadbeat anti-windup observer. The right-bottom diagram is a magnification of the left-bottom diagram in the region around the point -1.

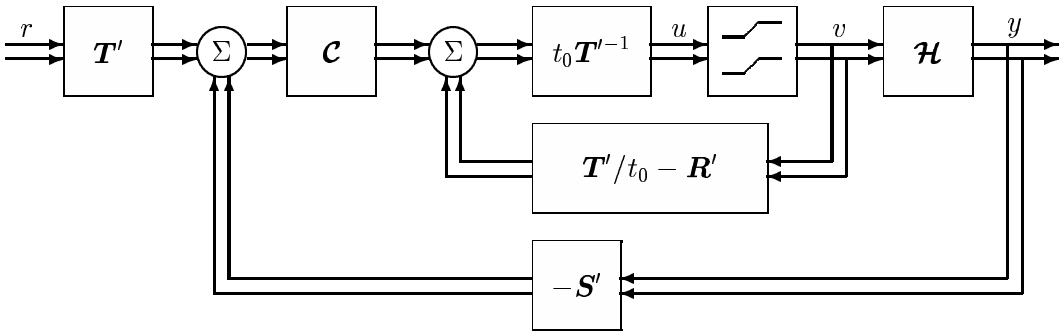

Figure 4.7: Feedforward-decoupling controller, with anti-windup compensation analogous to the conditioning technique, in conjuction with a process plant $\boldsymbol{\mathcal{H}}$.

Example 3

The anti-windup compensator used in this example corresponds to the Conditioning technique anti-windup compensator suggested in [2]. The control law is given by

$$(\boldsymbol{T}'/t_0)u = (\boldsymbol{T}'/t_0 - \boldsymbol{R}')v + \boldsymbol{\mathcal{C}}(-\boldsymbol{S}'y + \boldsymbol{T}'r) \quad . \tag{4.34}$$

Figure 4.7 illustrates the system. This compensated control law can also be seen as a special case of the more general anti-windup control law

$$u = (\mathbf{I}_2 - \boldsymbol{\mathcal{W}}\boldsymbol{R})v + \boldsymbol{\mathcal{W}}(-\boldsymbol{\mathcal{S}}y + \boldsymbol{\mathcal{T}}r) \quad . \tag{4.35}$$

Chosing $\boldsymbol{\mathcal{W}}$ as

$$\boldsymbol{\mathcal{W}} = \frac{1}{T'/t_0}\mathbf{I}_2 \tag{4.36}$$

will make (4.34) and (4.35) equal.

Evaluation of the simulation

The pre-existing controller, $\{\boldsymbol{R}', \boldsymbol{S}', \boldsymbol{T}'\}$, and the decoupling link $\boldsymbol{\mathcal{C}}$ are the same as in Example 1.

This system behaves nicely even though there is an intersection between the loop gain curve and the NLCF (bottom diagrams in Figure 4.8). Compared to the behaviour of the output signals in Example 2, this system acts real nice (upper diagram of Figure 4.8). The reason for this is that the intersection point is located further to the left in this case, than it was in Example 2. As a result, there must be higher amplitudes present in this loop in order to exite oscillativ modes. Still, there is no guarantee for the absence of nonlinear oscillations in this system.

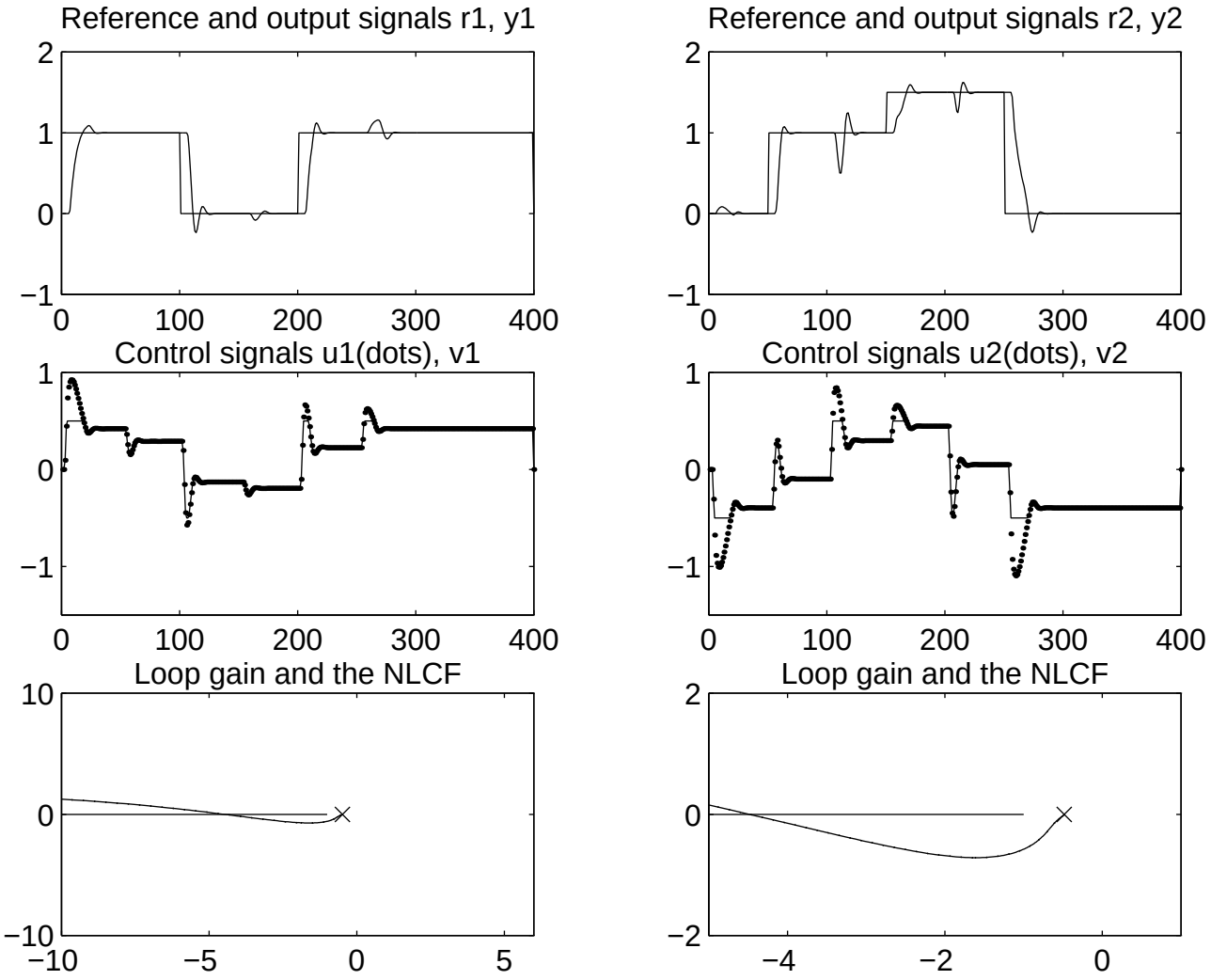

Figure 4.8: The HOF process controlled by a feedforward-decoupling LQ controller equiped with an anti-windup compensator based on the conditioning techique. The right-bottom diagram is a magnification of the left-bottom diagram in the region around the point -1.

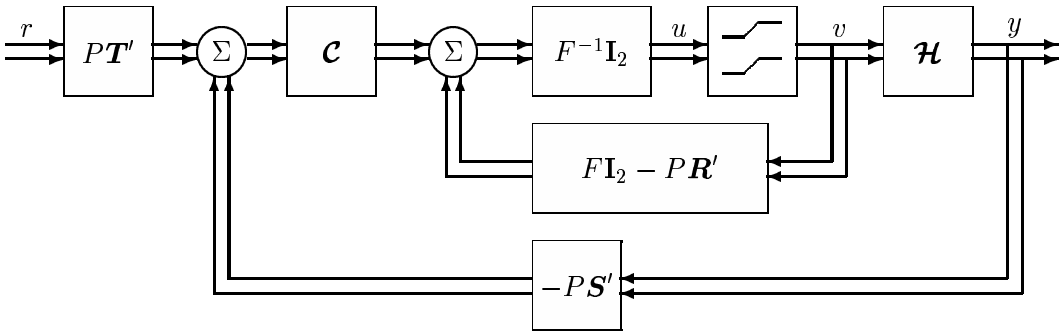

Figure 4.9: Feedforward-decoupling controller with modified systematic anti-windup compensation in conjuction with a process plant $\boldsymbol{\mathcal{H}}$.

Example 4

In this and also in the last example, the modified Systematic anti-windup design strategy, discussed earlier in this Chapter, is used for the design of the anti-windup compensator

$$\boldsymbol{\mathcal{W}} = \frac{P}{F}\mathbf{I}_2 \quad . \tag{4.37}$$

The stable polynomial F is then given by (4.27). The stable polynomial P is obtained from (4.28) where the trade-off parameter $\rho = 1$ in this example. Hence, the anti-windup compensated control law is

$$F\mathbf{I}_2 u = (F\mathbf{I}_2 - P\boldsymbol{R}')v + \boldsymbol{\mathcal{C}}(-P\boldsymbol{S}'y + P\boldsymbol{T}'r) \quad . \tag{4.38}$$

Figure 4.9 illustrates the system.

Evaluation of the simulation

The pre-existing controller, $\{\boldsymbol{R}', \boldsymbol{S}', \boldsymbol{T}'\}$, and the decoupling link $\boldsymbol{\mathcal{C}}$ are the same as in Example 1.

Regarding the shape of the loop gains and the behaviour of the output signals, this anti-windup compensation seems to have much in common with that used in Example 3. The loop gains (bottom diagrams in Figure 4.10) are almost identical to those in Example 3 (bottom diagrams in Figure 4.8). Note that the control signals $u1$, $u2$ (middle diagrams in Figure 4.10) both have larger amplitudes during the saturations event than the corresponding control signals $u1$, $u2$ in Example 3. But, as we can see, the saturated control signals in this example, are saturated under a less number of samples. In other words, the number of dots, during a saturations event in $u1$ in this example, are less then the number of dots during the same saturation event in $u1$ in Example 3. The same is true also for $u2$. Nevertheless, these two systems show almost identical behaviour.

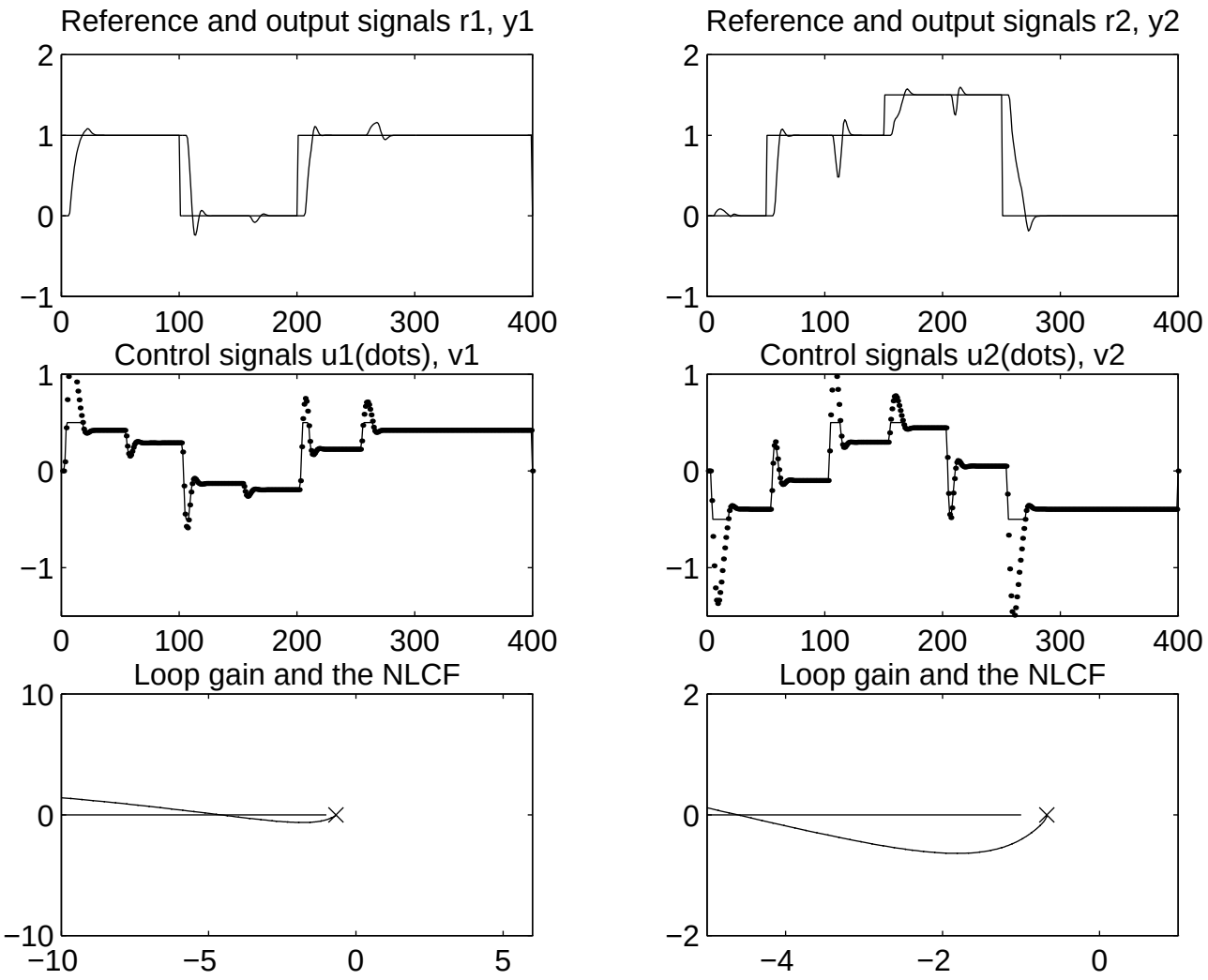

Figure 4.10: The HOF process controlled by a feedforward-decoupling LQ controller supplied with the modified systematic anti-windup compensation. The right-bottom diagram is a magnification of the left-bottom diagram in the region around the point -1.

Example 5

This system is identical to the one in Example 4 except for the fact that P is obtained from (4.28) with $\rho = 9$.

Evaluation of the simulation

As in the previous examples, the pre-existing controller, $\{\boldsymbol{R}', \boldsymbol{S}', \boldsymbol{T}'\}$, and the decoupling link $\boldsymbol{C}$ are the same as in Example 1.

The loop gain curve does not intersect the NLCF and the output signals behave nicely. As we can see in the middle diagrams of Figure 4.11, the number of time instants when the control signal saturates, is less than in any of the Examples 2-4. Compared to the system in Example 1, this is not the case. The difference in the behaviour of the control signals in this Example and the control signals in Example 1, is that those in Example 1 tends to oscillate soon after the desaturation events. As a result, desaturation transients will be present for a longer time in that system. These effects can be explained by the loop gain and the shape of the loop gain curves. The loop gain is "higher" in this example than in Example 1, i.e. the loop gain curves in the lower diagrams of Figure 4.11 are more "blown up" than those in Figure 4.4 and hence, the desaturation transients will decay faster in this system.

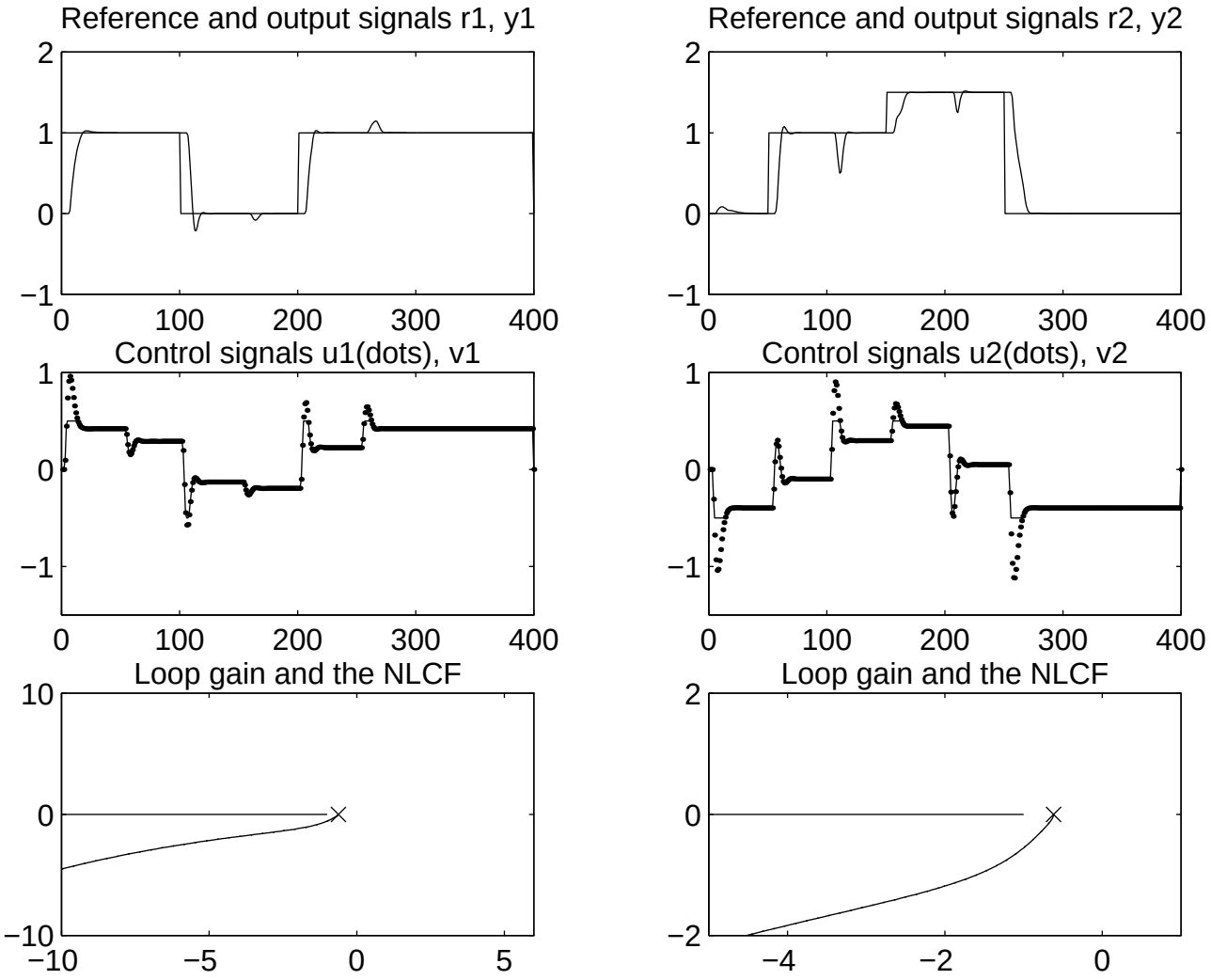

Figure 4.11: The HOF process controlled by a feedforward-decoupling LQ controller supplied with the modified systematic anti-windup compensation. The right-bottom diagram is a magnification of the left-bottom diagram, in the region of the point -1.

4.3.1 Summary of the simulation results

Let us first conclude that the nominal system in Example 1 performed quit well under the present conditions. But, as mentioned in the begining of this report, there is no guarantee for a satisfactory behaviour, during or after a saturation event, of such a system. There are many factors involved which may have a bad influence on the performance of any system, during or after a saturation event. The dynamic properties of the plant, the constraints of the actuator and the design of the nominal controller, are some important factors. If we had used another regulator, without anti-windup compensation, for the control of the HOF process in Example 1, then that system may not have performed as well. Compared to the pre-existing $\{\boldsymbol{R}', \boldsymbol{S}', \boldsymbol{T}'\}$ regulator that we used in all the examples, such a regulator may have been designed by use of a lower penalty on the control signal increment and/or an observer pole located closer to the origin. How the anti-windup compensated controllers in the Examples 2 and 3 had performed with such a pre-existing controller is not easy to anticipate, but one thing is clear; regarding control signal saturation events, there is no guarantee for a satisfactory behaviour of such systems either.

If that pre-existing regulator had been used in the Examples 4 and 5, it still had been possible to obtain loop gains which shapes had been almost identical to those in Example 5.

Chapter 5

Conclusions

In Chapter 3 we suggested a method for anti-windup compensation of multivariable controllers. It is a generalization of the Systematic anti-windup design method, developed and discussed in [6] for scalar systems. Therefore, a brief description of that method was presented in Chapter 2. We showed that the multivariable anti-windup design could be reduced to a set of scalar designs, by diagonalizing the loop gain around the control signal saturation elements. The scalar loop gains could then be adjusted so that the desaturation transients in the output signals, decay fast, while nonlinear oscillations are avoided. For a system with m inputs (inputs to the plant) this design requires that m scalar penalties are chosen appropriately.

Anti-windup compensation of feedforward decoupling controllers, used to control MIMO processes, where discussed in Chapter 4. A number of simulations of such a decoupled system, using different anti-windup compensation strategies, where also presented and discussed in Chapter 4. Unfortunatly, the general method developed in Chapter 3 has not yet been evaluated by simulations. A complete investigation of the general method discussed in Chapter 3 and also an investigation of how the limitation in the control signal *increment* could be taken into account in the anti-windup design, are important topics for futhure research.

Bibliography

[1] K.J. Åström, and B. Wittenmark, *Computer-Controlled Systems.* Englewood Cliffs, NJ: Prentice-Hall, 1990.

[2] R. Hanus, M. Kinnaert and J-L. Henrotte, "Conditioning technique, a general anti-windup and bumpless transfer method," *Automatica,* vol. 23, pp. 729-739, 1987.

[3] S. Rönnbäck, *Linear Control of Systems with Actuator Constraints.* PhD thesis, Division of Automatic Control, LuleåUniversity of Technology, Sweden, 1993.

[4] Ch. Wurmthaler and P. Hippe, "Systematic compensator design in the presence of input saturation," *Proceedings of the ECC '91,* Grenoble, France, July 2-5, pp. 1268-1273.

[5] S. Rönnbäck, K.S. Walgama and J. Sternby, "An extension to the generalized anti-windup compensator," *Proceedings of the 13th IMACS World Congress on Computation and Applied Mathematics,* Dublin, Ireland, 3, pp. 1192-1196.

[6] M. Sternad and S. Rönnbäck, "A Frequence domain approach to anti-windup compensator design," Inst. Technol., Uppsala Univ., Sweden, Rep. UPTEC 93024R, 1993.

[7] G. Torkel and L. Ljung, *Reglerteknik Grundläggande teori.* Studentlitteratur, 1989.

[8] D.P. Atherton, *Nonlinear Control Engineering.* Van Nostrand, London, UK, 1975.

[9] T. Kailath *Linear Systems.* Englewood Cliffs, NJ: Prentice-Hall, 1980.

[10] J.M. Maciejowski *Multivariable Feedback Design.* Addison Wesley, Reading, Mass, 1989.

[11] M. Sternad and A. Ahlen, "A novel derivation methodology for polynomial-LQ controller design," *IEEE Transactions on Automatic Control,* vol. 38, pp. 116-121, 1993.